AALBORG UNIVERSITY
DENMARK

Selective electrical stimulation of peripheral nerve fibers

accommodation based methods

Hennings, Kristian

Publication date:
2004

Document Version
Publisher's PDF, also known as Version of record

Selective Electrical Stimulation of Peripheral Nerve Fibers: Accommodation Based Methods

Ph.D. Thesis

Kristian Hennings

2004

Laboratory for Experimental Pain Research

Center for Sensory-Motor Interaction (SMI)

Frederik Bajers Vej 7 DK-9220 Aalborg Denmark

Phone: +45 96 35 88 18

Fax: +45 98 15 40 08

Preface

This Ph.D. thesis is the result of work carried out at the Center for Sensory-Motor Interaction, Aalborg University and at the Faculty of Dentistry, University of Toronto in the period from 2001 to 2004. The project was motivated by the idea of using and adapting accommodation-based methods for selective electrical stimulation of motor fibers to the study of the human nociceptive system. This has not been without difficulties, but it has still been a rewarding process, as it has provided the opportunity to study interesting biophysical mechanisms and to enhance the understanding of accommodation based methods. Throughout this project, I am indebted to all the co-workers and friends at the Center of Sensory Motor Interaction and at the Faculty of Dentistry, University of Toronto that I have had the fortune to work with and learn from. I wish to express my sincerest gratitude to my supervisor Associate Prof. Ole K. Andersen and Professor Lars Arendt-Nielsen, the head of Center for Sensory Motor Interaction, for their never failing interest and enthusiasm. I will also like to express my deepest gratitude to my hosts at the Faculty of Dentistry, University of Toronto, Professor Barry J. Sessle and Professor James W. Hu. Furthermore, I will like to thank Dr. Alexandra Vuckovic for graciously offering her volume conductor model for my study on exponentially rising waveforms, and Dr. David Lamb for his patience and skill in teaching an engineer to do complicated surgery. Finally, I will like to thank my wife Laura Hennings for her love and support, without her this project would not exist.

Aalborg, December 2004

List of papers

This Ph.D. thesis is based on four papers, which are referred to with Roman numerals:

I.   Hennings K, Arendt-Nielsen L, Christensen SS, and Andersen OK. Selective activation of small diameter motor fibers using exponentially rising waveforms: a theoretical study. Med Biol Eng Comput 2005. Jul;43(4):493-500. doi: 10.1007/BF02344731

II.   Hennings K, Hu JW, Sessle BJ, Arendt-Nielsen L, and Andersen OK. Effect of rectangular sub-threshold prepulses on the electrical recruitment order of nerve fibers. (In preparation)

III.   Hennings K, Arendt-Nielsen L, and Andersen OK. Orderly activation of human motor neurons using electrical ramp prepulses. Clin Neurophysiol 2005. Mar;116(3):597-604. doi:10.1016/j.clinph.2004.09.011

IV.   Hennings K, Arendt-Nielsen L, and Andersen OK. Breakdown of accommodation in nerve: a possible role for persistent sodium current. Theor Biol Med Model 2005. Apr 12;2:16. doi:10.1186/1742-4682-2-16

Abstract

In this thesis, accommodation based methods for selective activation of nerve fibers and underlying biophysical mechanisms were investigated both experimentally and theoretically. In the experimental studies, animal and human experiments were used to study the effect of rectangular (paper II) and ramp prepulses (paper III) on the recruitment order of motor and sensory fibers, respectively. In the theoretical studies, nerve fiber models (paper I) were used to study a new method termed exponentially rising waveforms and breakdown of accommodation (paper IV).

In paper I, it was found that exponentially rising waveforms in theory can reverse the recruitment order of large ($15.5\mu m$) and small ($8\mu m$) nerve fibers. This reversal was explained by differences in the second order difference quotient of the membrane potential (termed a deactivating function) between large and small nerve fibers. In paper II, rectangular prepulses (1ms, 10ms, and 100ms in duration) were observed in rat experiments to change the recruitment order of sensory fibers. However, there were not observed a significant difference in the recruitment order of sensory fibers between the different rectangular prepulses. In paper III, ramp prepulses were in human experiments observed to change the recruitment order of α-motor fibers and breakdown of accommodation was observed for ramp pulses. In paper IV, it was found that persistent sodium current could explain this breakdown of accommodation in motor fibers (i.e. that long duration slowly rising stimuli activates nerve fibers at a near constant intensity, no matter how slowly this intensity is approached).

In conclusion, the present work has provided biophysical explanations for selective activation of small motor fibers with exponentially rising waveforms (deactivating function) and breakdown of accommodation (persistent sodium current). Rectangular and ramp prepulses were observed to change the recruitment order of relative homogeneous fiber groups (large sensory fibers and α-motor fibers). However, the observations on breakdown of accommodation (paper III and IV), suggests that accommodation based methods cannot be used to change the recruitment order of two distinct fibers groups (such as myelinated and nonmyelinated nerve fibers). Paper IV, suggests that breakdown of accommodation can be used as a tool for studying persistent sodium channels under normal and pathological conditions.

Synopsis

I denne afhandling er akkommodations baserede metoder til selektiv elektrisk stimulering samt underliggende biofysiske mekanismer blevet undersøgt både eksperimentelt og teoretisk. I de eksperimentelle studier er der benyttet både dyre og human forsøg til at bestemme virkningen af firkantede (artikel II) og lineært stigende prepulser (artikel III) på rekrutteringsordenen af henholdsvis motoriske og sensoriske nerve fibre. I de teoretiske studier er nerve fiber modeller blevet brugt til at undersøge en ny metode kaldet eksponentielt stigende kurveformer (artikel I) og til at undersøge nedbrud af akkommodation (artikel IV).

I artikel I blev der observeret en reversering af rekrutteringsordenen af store (15.5μm) og små (8μm) nerve fibre. Denne reversering blev forklaret med forskelle imellem den anden ordens differens kvotient af membran potentialet (defineret som en deaktiverings funktion) for store og små nerve fibre. I artikel II blev der i rotte forsøg observeret en ændring a rekrutteringsordenen for store sensoriske fibre med firkantede prepulser (længde: 1ms, 10ms, 100ms). Men der blev ikke observeret en signifikant forskel i rekrutteringsordenen imellem de forskellige prepulser. I artikel III blev der i human forsøg fundet en ændring af rekrutteringsordenen for motoriske nerve fibre med lineært stigende prepulser og nedbrud af akkommodation blev observeret for lineært stigende pulser. I artikel IV blev dette nedbrud af akkommodation i motoriske nerve fibre forklaret med natrium kanaler uden deaktivering.

Det konkluderes at denne afhandling har tilvejebragt biofysiske forklaringer på selektiv aktivering af små motoriske nerve fibre med eksponentielt stigende kurveformer (deaktiverings funktioner) og nedbrud af akkommodation (natrium kanaler uden deaktivering). Firkantede og lineært stigende prepulser kan ændre rekrutteringsordenen af relativt homogene nerve fiber grupper (store sensoriske nerve fibre og motoriske nerve fibre). Men observationerne af nedbrug af akkommodation indikerer at akkommodations baserede metoder ikke kan ændre rekrutteringsordenen af meget forskellige nerve fiber grupper (såsom myeliserede og ikke myeliserede nerve fibre). Artikel IV foreslår at nedbrug af akkommodation kan bruges til at studere natrium kanaler uden deaktivering under normale og patologiske omstændigheder.

Table of contents

1 Introduction

Electrical stimulation is a method for evoking artificial activity in the nervous system and it has found its use within diverse fields, such as rehabilitation technology (78) and clinical neurophysiology (31). However, neural activation with electrical stimulation is indiscriminant (40;78) and as a consequence the nervous system reacts to electrical stimulation with activity that has little or no resemblance with natural occurring stimuli. On the other side, electrical stimulation, have advantages that have outweighed its indiscriminate neural activation, which is its ease of application, high-temporal resolution, and reproducibility.

In rehabilitation technology, functional electrical stimulation (FES) has been used to restore motor control in patients with spinal cord injury or stroke, but this restoration has been limited in many cases. The control of the muscle is coarse and the muscles fatigue rapidly, due to the type of neural activity evoked by FES the (92). As a result, with coarse muscle contractions, it is difficult to achieve the delicate movements that are necessary for daily life activities (e.g. eating, drinking, or writing) and the fatigue of electrically evoked muscle contractions makes it difficult to maintain large-scale movements (e.g. walking or cycling).

In clinical neurophysiology, electrical stimulation can be used to estimate the nerve conduction velocity (NCV) and other measurements of neuromuscular function. These measures obtained with electrical stimulation are of great diagnostic value as it is abnormal in many neurogenic and myogenic disorders, but there are exceptions. One example is myopathies, where the NCV is often found to be normal. Instead, conventional needle electromyography are important for the diagnosis of myopathies, where motor unit action potentials (MUAP) are recorded and examined while the patients is performing low levels of voluntary contractions. This method has shortcomings; some persons cannot fire only one or two MUAPs at minimal voluntary contractions (31) and the technique can only evaluate myopathies that effect type I motor units (motor units recruited at low levels of voluntary contractions (45)). Consequently, the technique may not be possible to perform in all persons, and it may insensitive to myopathies that effect type II motor units (e.g. steroid myopathy) (31).

Some of the limitations and shortcomings of FES and needle electromyography may be overcome with the use of selective electrical stimulation. The aim of this selective electrical stimulation is to control the electrically evoked neural activity. This may allow finely graded non-fatigable muscle contractions in FES and may facilitate new methods for recording and examination of multiple single motor units in needle electromyography for the diagnosis of myopathies.

1.1 Recruitment order with conventional electrical stimulation

The action potentials initiated by electrical stimulation are indistinguishable from "natural" action potentials for the target organs, such as muscles or nerve cells in the central nervous system (CNS). Natural occurring action potentials are initiated by receptor or synaptic potentials at either the trigger zone or the axon hillock, where after these action potentials are conducted orthodromically along the axons (53).

In electrical stimulation, action potentials are instead initiated where axons pass near to stimulating electrodes by electrically evoked changes in the extra-cellular potential field (67). This change in the extra-cellular potential field is caused by the passing of electric current through the tissue leading to axon depolarization at the cathode and hyperpolarization at the anode. Whether the current will initiate action potentials in a nerve fiber depends on whether the current is below or above its excitation threshold. A nerve fiber's excitation threshold is determined by a number of factors, for example its; type (sensory or motor) (73), diameter (14;67;76;77), and position with respect to the stimulating electrode (42;70). With regard to the position of the nerve fibers, it has been found that nerve fibers close to the electrode are activated at lower stimulus intensities than more distant nerve fibers (40).

There is an extensive body of knowledge on the relation between nerve fiber diameter and type (e.g. α-motor fibers, mechanoreceptive fibers, pain fibers, etc.). Consequently, the effect of electrical stimulation can partially be predicted by knowing its recruitment order with respect to nerve fiber diameter. In animal studies large diameter nerve fibers have invariantly been recruited before small diameter nerve fibers by electrical stimulation (14;33;34), and modeling studies have provided a theoretical explanation for this observation. From models of myelinated nerve fibers, the second order difference quotient of the extra-cellular potential has been identified as the most important factor in determining the excitability of a nerve fiber (76;77). As, this second order difference quotient is proportionally related to the inter-nodal distance and the inter-nodal distance is proportionally related to nerve fiber diameter (71) this forms the mechanism by which conventional electrical stimulation recruit large before small nerve fibers.

The recruitment of large before small nerve fibers by electrical stimulation, has been labeled as an inverse recruitment order, since it implies that large motor units are recruited before small motor units by electrical stimulation, which is the inverse of the normal physiological recruitment order of motor units (orderly recruitment) (45). This inverse recruitment order has invariantly been observed in animal experiments; however, these observations have been challenged by observations in human experiments. Human experiments with both motor point and direct nerve stimulation of muscles have resulted in

conflicting results. In one study on motor point stimulation, an inverse recruitment order was observed (103). Three other studies have found a preferentially orderly recruitment order with motor point stimulation (35;57;69), which have been suggested to be due to a higher percentage of type II motor units in center of the muscle (57;69) (which has been found by Helliwell et al. (1987) (44) and Henriksson-Larsen et al. (1985) (47)).

There is less data on direct nerve stimulation, however, two studies have shown an orderly recruitment of motor neurons with direct nerve stimulation (101) (39). The observation of an orderly recruitment order with direct nerve stimulation is controversial as it challenges the established explanation of the high fatigue of muscles with electrical stimulation that this fatigue is due to a preferential activation of type II motor units with electrical stimulation. It was found that the orderly recruitment with direct nerve stimulation could not be explained by large motor neurons being located deeper in the nerve than small motor neurons, and instead it was suggested to be due to different membrane properties of type I and II motor neurons (101). The membrane properties of type I and II motor neurons have been found to differ between the two types (111), however, the results of the two studies on direct nerve stimulation may have been biased by the techniques used in these studies.

The two studies on direct nerve stimulation used twitch force (101) and fatigability (39) of the activated motor units in paralyzed or partially paralyzed thenar muscles as indices of the recruitment order. In using twitch forces as indices of the recruitment order, it is assumed that there is a positive correlation between the conduction velocity and the twitch force of a motor unit. This relationship has been clearly demonstrated in animal studies on heterogeneous muscles (24;68;111). However, studies on healthy human thenar muscles are conflicting. A positive correlation between conduction velocity and twitch force has been demonstrated in one study (27) and in another study no correlation has been found (100). Furthermore, in a study on paralyzed thenar muscles presented evidence for a greater atrophy and weakening of type II motor units than of type I motor units (99). Consequently, the recruitment of weak before strong motor units in paralyzed muscle does not necessarily imply an orderly recruitment order of motor neurons with direct nerve stimulation.

The use of fatigability of as an index of recruitment order (39) may be biased by confounding factors. The recruitment order was inferred from the different fatigability of a part of the muscle compared to the whole muscle. In this comparison other factors than the type of the activated motor units may play a role in the observation of a difference in the fatigability, such as temperature, extra-cellular concentration of calcium, and blood flow occlusion. However, there is little data available for assessing the influence of these confounding factors on the use of fatigability as an index of recruitment order.

5

The observation of an orderly recruitment order of motor neurons is in disagreement with the established theory on electrical stimulation (67;76;77;79), and although these findings may be disputed by various confounding factors, they also demonstrate that the question of the recruitment order of motor neurons with surface electrodes is less closed than previously assumed.

1.2 Methods for selective electrical stimulation

Methods for controlling the recruitment order of electrical stimulation have been the focus of several studies. The aim has been to recruit small before large motor neurons or distant motor neurons before motor neurons close to the stimulating electrode. In these methods, experimental setups with two stimulating electrode have been used for selective activation of small motor neurons using collision techniques (50;51;83), block with direct current (38;65;88;102;112), and block with high frequency stimulation (8;22;56;92;97). With one stimulating electrode, selective activation of small motor neurons has been achieved using anodal blocking (1;33;34;81;82;96;107), slowly rising waveforms (63), and sub-threshold prepulses (15;28;29;41;75;105).

1.2.1 Collision techniques

Collision techniques can be used for estimating the conduction velocity distribution of a motor nerve, and are known as Hopf's and Ingram's technique (50)(cf. Ruijten et al. (1993) (83) for a description of Hopf's technique). These techniques use a two-point stimulation of nerves at a distal and proximal site and paired distal and proximal supra-maximal stimuli with variable inter-stimulus-intervals (ISI) (see **Figure 1**).

In Hopf's technique, the conduction velocity of the slowest nerve fiber in a test response is known by evoking it with a distal stimulus paired with a subsequent proximal stimulus, where the test responses is the response from the proximal stimulus. For short ISIs the responses from the distal and proximal stimuli collide completely and there is no test response (the 65m/s response in **Figure 1**). When the ISI is increased, the fastest action potentials from the distal stimulus will have propagated past the proximal site. The proximal stimulus will then re-excite these nerve fibers, and a test response can be observed (60m/s to 30m/s responses in **Figure 1**). The limit for the slowest nerve fibers in the test response can be determined from the distance between the distal and proximal site and the ISI.

In Ingram's technique, the sequence of the distal and proximal stimulus is reversed and they are paired with a third proximal stimulus that collides with the test response from Hopf's technique. Ingram's technique results in test responses that contain only slow nerve fibers with a known conduction velocity of the fastest nerve fiber in the responses (50). Neither Hopf's or Ingram's technique is a true selective

electrical stimulation, as the responses from the stimuli will contain the whole population of nerve fibers. However, these techniques are interesting as the responses from small nerve fibers can be obtained with subtraction techniques and there is a direct relationship between the ISI parameter and the conduction velocities of the nerve fibers in the test response.
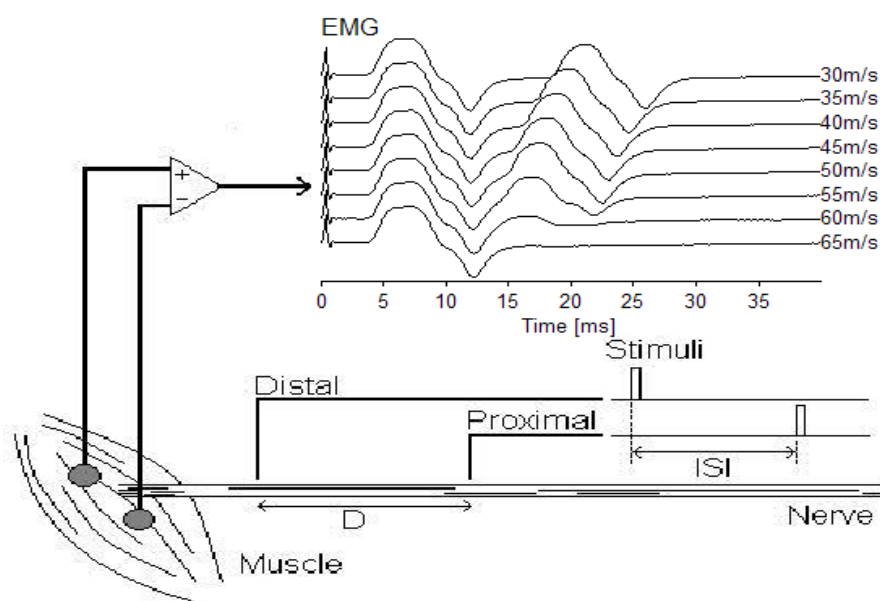

Figure 1: Illustration of Hopf's technique in which a distal and proximal stimulus with a variable inter-stimulus-interval is used for evoking a test response containing only fast nerve fibers. The EMG shown in the illustration is obtained from the thenar muscles and with stimulation of the median nerve at the wrist and the elbow. Please observe how the test response (the second CMAP volley) is absent for the smallest ISI (65m/s) and how it is gradually increased when the ISI is increased (lower CV). From the data shown in this illustration, it was estimated that the subject had a range of motor neuron CVs between 35m/s to 65m/s.

1.2.2 High frequency stimulation and direct current

High frequency stimulation and direct current can be used with two stimulating electrodes to selectively block the propagation of action potentials in large nerve fibers. In these methods, one of the electrodes is used to excite all of the nerve fibers and the second is used for blocking the large nerve fibers with high frequency stimulation or direct current of sufficient intensity. This is possible, as both high frequency stimulation and direct current have been shown to block progressively smaller nerve fibers with an increase in stimulus intensity (8;88;92;97;112). The blocking of nerve fibers with direct current has been explained by membrane depolarization and associated sodium channel inactivation (88). However, evidence has also been found for anodal blocking to be one of the underlying mechanisms, as activity due to the direct current has been observed, which was abolished when the blocking anode was placed closest to the recording electrodes (65). With high frequency stimulation the block of motor neurons has been explained by both a conduction block of the nerve fibers (22;56) or by depletion and failure of reuptake of acetylcholine at the motor endplate, which prevents it to follow the high firing rates induced by the high frequency stimulation (8;92). The disagreements on the underlying mechanism for high frequency stimulation may be a result of the different stimuli that have been used in high frequency

stimulation experiments so far. Hence, sinusoidal waveforms (1kHz – 20kHz) (22;56;97) and bipolar and monopolar rectangular pulses (600Hz) (8;92) have all been used for high frequency stimulation (see Kilgore and Bhadra (2004) for a review). With sinusoidal waveforms (> ~1kHz), depletion of the motor endplate cannot explain the block with high frequency stimulation as stimuli delivered to the nerve between the blocking electrode and the muscle results in the same contractions as when the high frequency stimulation is absent (56).

1.2.3   Anodal Blocking

Anodal blocking can be used to block propagation of action potentials in large nerve fibers, and thus create a selective activation of small nerve fibers. In electrical stimulation, nerve fibers become depolarized under cathodes and hyperpolarized under anodes. At supra-threshold stimulation intensities action potentials are initiated by the depolarization at the cathode. However, when stimulation intensities are increased well above the nerve fibers' threshold the hyperpolarization at the anode becomes strong enough to block the action potentials generated at the cathode. Anodal blocking may be used for selective activation small nerve fibers, as the threshold at which anodal block occurs in a nerve fiber is inversely related to its diameter. This inverse relationship between the threshold for anodal blocking and nerve fiber diameter is due to the larger depolarization and hyperpolarization by electrical stimuli of large nerve fibers as compared to small nerve fibers. The discovery of anodal block is accredited to Pflüger who found in 1858 that the onset of strong pulses failed to cause contractions in frog gastronemius preparations due to a failure of the action potential to propagate pass the anode (as cited by Accornero et al. (1977)). Anodal block was first used for selective electrical stimulation by Kuffler and Vaughan-Williams (1953) who used rectangular pulses to induce anodal blocking in frog motor nerves (61). They adjusted the stimulus duration so it would block the fast nerve fibers but would allow the action potentials in the small nerve fibers to propagate. With this method, they were capable of generating selective electrical stimulation of small nerve fibers. The method of Kuffler and Vaughan-Williams (1953) is highly attractive, as there is a direct relationship between stimulus parameters and the conduction velocity of the largest activated nerve fiber, which can be calculated from the distance between the cathode and anode and the duration of the stimulus. Unfortunately, the method of Kuffler and Vaughan-Williams (1953) is not applicable to mammalian nerve due to anodal break excitation, which occurs at the cessation of intense stimuli. Anodal break excitation will re-excite the blocked large nerve fibers and will thereby prevent a selective activation of small nerve fibers. To overcome the problem of anodal break excitation both triangular (1) and quasi-trapezoidal (33;34) pulses have been proposed. Triangular and quasi-trapezoidal pulses prevent anodal break excitation with an exponential trailing phase. Thereby, the pulses do not have the abrupt cessation of the current that is the cause of anodal break excitation. With the Triangular and quasi-trapezoidal pulses the extend of the block can

only be modulated by the intensity of the stimulation and not its duration as the cessation of pulse is not clearly defined, as it is with rectangular stimuli. Consequently, with these pulses there are no direct relationship between stimulus parameters (intensity and duration) and the maximum conduction velocity in the response. Anodal blocking has theoretically been shown to work with a monopolar point electrode (81), which suggests that this technique may be used with surface electrodes. However, anodal blocking does not appear in nerve conduction studies, and seam only to work with hook, cuff or similar electrodes (30).

1.2.4 Slowly Rising Waveforms

Slowly rising waveforms have been shown to recruit motor units in the same order as during voluntary contractions (63). This was observed in a study using intramuscular recording with needle electrodes of single motor units and classification of the motor units based on their peak-to-peak amplitude during electrically and voluntary elicited muscle contractions of increasing intensities. This study was made before Hodgkin's and Huxley's description of the biophysical basis for the action potential (49). Kugelberg and Skoglund (1946) were, therefore, unable to provide a biophysical explanation for the orderly recruitment of motor neurons with slowly rising waveforms. Today, this biophysical explanation is still unresolved and the experiment has not been reproduced.

1.2.5 Sub-threshold Prepulses

Sub-threshold prepulses change the excitability of nerve fibers to a subsequent stimulus. A depolarizing sub-threshold prepulse is considered to change the excitability of nerve fibers by inactivation of sodium channels (41) or by activation of potassium channels (3). This change in excitability is voltage dependent and is therefore proportional to the intensity of the sub-threshold prepulse (41). Normally, large nerve fibers are depolarized more by electrical stimuli and consequently have lower excitation thresholds (67). However, this relation also implies that large nerve fibers are depolarized more by sub-threshold prepulses than smaller nerve fibers and consequently that the excitability of large nerve fibers is changed more than the excitability of smaller nerve fibers. The same relations are valid for nerve fibers close to the stimulation electrode and nerve fibers that are more distant to the stimulation electrode. In the method of sub-threshold prepulses, the change in excitability is thought to increase the excitation thresholds of large nerve fibers more than the excitation thresholds of small nerve fibers and this change is theoretically determined by sodium channel inactivation (28;29;40;41). Consequently, sub-threshold prepulses have the potential of both activating small and distant nerve fibers selectively without simultaneous activation of large nerve fibers and nerve fibers close to the stimulation electrode (41).

Experimental evidence for the ability of sub-threshold prepulses to selectively activate distant nerve fibers has been found by measurement of joint torque (plantar-flexion/dorsiflexion) and stimulation of the cat sciatic nerve (41) and by measurement of pain thresholds in human subjects (75). In the study of Grill and Mortimer (1997) on cat sciatic nerves, sub-threshold prepulses inverted the recruitment order of plantar-/dorsiflexor muscles (41), and in the study of Poletto and van Doren (2002) humans sub-threshold prepulses have been observed to elevate pain thresholds in stimulation with small needle electrodes (75). Small needle electrodes preferentially activate superficial Aδ and C fibers (70). Consequently, the elevated pain thresholds with sub-threshold prepulses suggests that the prepulses reversed the recruitment order of superficial Aδ/C fibers and Aβ fibers located deeper within the skin. The ability of sub-threshold prepulses to selectively activate small motor neurons has been studied by Bolhuis et al. (2001) using the muscles twitch forces. With sub-threshold prepulses the twitch forces were observed to have longer relaxations times as compared to rectangular stimuli alone, which indicated that slow fatigue-resistant motor units were selectively activated with the sub-threshold prepulses (105).

1.3 Aim of the Ph.D. project

The aim of this Ph.D. project was to study methods for selective electrical stimulation that are based on accommodation of nerve fibers, and related underlying biophysical mechanisms. These methods included exponentially rising waveforms and sub-threshold prepulses. The present thesis is concerned with a number of unresolved questions related to these methods, which have been addressed in both theoretical (models of motor axons) and experimental (human and animal experiments) studies. These studies has been organized into four papers (I – IV):

In paper I, a computer model was used to study exponentially rising waveforms. The paper focused on providing a biophysical explanation for selective electrical stimulation with exponentially rising waveforms and to determine the relationship between stimulus parameters and the recruitment order of nerve fibers when they are stimulated with a cuff electrode (Chapter 4). In paper II, an animal model was used to study the recruitment order of nerve fibers with rectangular prepulses, and in paper III, human experiments using surface electrodes was used to study the recruitment order of nerve fibers with ramp prepulses (Chapter 5). In paper IV, a model of space-clamped motor axon was used to study the biophysical mechanism for breakdown of accommodation and how it can be simulated with computer models (Chapter 6).

Throughout the thesis, these papers are referred to with roman numerals (I – IV).

2   Methods used in the studies

2.1   Exponentially rising waveforms (paper I)

2.1.1   Background

The study on exponentially rising waveforms (paper I) was motivated by the observation of Kugelberg and Skoglund (1946) that slowly rising waveforms recruits motor neurons in same order as voluntary contractions (63). However, the study of Kugelberg and Skoglund (1946) needs to be extended, due to technical limitations at the time of the study and due to how the results were reported. The slowly rising waveforms of Kugelberg and Skoglund (1946) consisted of a linearly rising phase that continued until the desired stimulus intensity was reached, where after the current was held constant until the cessation of the stimulus. Fast rise times could be generate automatically, but, slow rise times were controlled by hand and in these cases, the rising phases were only approximately linearly rising. However, they did not report the rise times and stimulus durations used to obtain orderly recruitment of motor neurons, which is needed for practical use. Furthermore, the underlying biophysical mechanism is unknown.

Paper I was based on the hypothesis that slowly rising waveform may selectively activate small nerve fibers. However, the study did not use the linearly rising waveforms used by Kugelberg and Skoglund (1946) but instead exponentially rising waveforms. The exponentially rising waveforms were defined by the following equation:

$$i(t) = \begin{cases} \dfrac{I_S}{e^{T_s\tau}-1}\left(e^{\frac{t}{\tau}}-1\right) & 0 \le t \le T_s \\[2em] I_s e^{-(t-T_S)}\text{)}0.15ms & T_S t \end{cases} \qquad (2)$$

with T_S the stimulus duration, τ time constant, and I_S the stimulus current. The exponentially rising waveform was chosen based on the description that nowadays are available for the generation of action potentials (49), which was unavailable to Kugelberg and Skoglund (1946). The slowly rising waveforms were hypothesized to work indirectly through accommodation of the nerve fibers to the stimuli (see section Deactivating Function for a more detailed discussion). At the onset of the slowly rising stimulus, the rate of rise has to be sufficiently slow so the stimulus will not excite the nerve fibers. However, as accommodation takes place during the stimulus, the rate of rise can be increased without causing an excitation of the nerve fibers. Consequently, based on this hypothesis, an exponentially rising waveform

were the slope is gradually increased during the stimulation may be advantageous to linearly rising waveforms.

A model of rabbit myelinated nerve fibers coupled with a volume conductor model for a nerve enclosed in a cuff electrode was used for studying the biophysical mechanism and recruitment order with exponentially rising waveforms.

2.1.2 Nerve Fiber Model

The nerve fiber model used to study exponentially rising waveforms was a McNeal-type compartment cable model (67). Instead of the original Frankenhauser-Huxley equations for the ionic currents it was based on data from rabbit myelinated nerve fibers (26), as they have been adapted for the body temperature of 37°C by Sweeney et al. (1987) (95). The parameters for the cable model were taken from the study of Deurloo et al. (2001) (28). This model has previously been used extensively to study the effect of electrical stimulation (41;42) (29;40;77;79).

The model of the motor axons was based on a description of a motor axon as an electrical equivalent circuit (see Figure 2). This representation is based on the assumption that the myelin has an insignificant conductance and capacitance. For a nerve fiber with diameter (D), the linear parameters of the model can be found as, nodal capacitance: $C_M = c_m \pi d l$ (c_m: membrane capacitance per unit area, l: length of the node (1.5μm), and d: axon diameter (0.6D)), and the intra-axonal conductivity is given as $G_A = \pi d^2/4\rho_i L$ (ρ_i: resistivity of the axo-plasm, and L: inter-nodal-distance (100*D)).
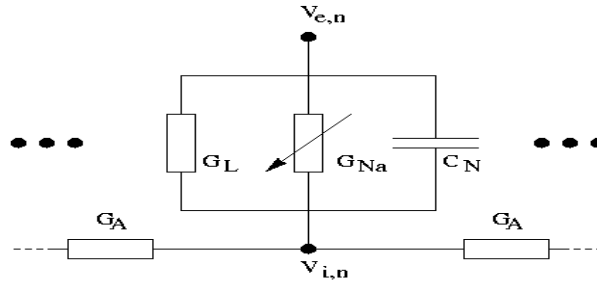
Figure 2: Illustration of the electrical cable model for myelinated motor neurons. At each node of Ranvier, the membrane is modeled as a membrane capacitance C_N in parallel with a linear leakage current $i_L = G_L(V_n-E_L)$ and a nonlinear sodium $i_{Na} = G_{Na}(V_n-E_{Na})$ currents. The E_L, and E_{Na} potentials are the Nernst potentials for the leakage and sodium currents, respectively. The sodium is a nonlinear function of time and membrane potential. The membrane potential V_n was given as the intra-cellular potential V_i minus the extra-cellular potential V_e. The intra-axonal conductance was modeled by a linear conductance G_A.

From the electrical equivalent circuit the following partial differential equation can be derived for the reduced trans-membrane potentials (V_n). Where V_n is given as $V_{i,n} - V_{e,n}$.

$$\frac{dV_n}{dt} = \frac{G_A}{C_M}\left(V_{n-1} - 2V_n + V_{n-1} + V_{e,n-1} - 2V_{e,n} + V_{e,n-1}\right) - \frac{\pi d l}{C_M}(i_{Na} + i_L) \qquad (1)$$

The ratios in equation (1) can be reduced to constants ($G_A/C_M = g_a/240c_m\rho_i l$, and $\pi l d/C_M = 1/c_m$), due to the linear relation between axon diameter and inter-nodal distance. Equation (1) reveals that with this model the only difference between nerve fibers of different diameter is the extra-cellular field (V_e). Furthermore, from equation (1) it can be seen that it is the difference in the extra-cellular potential ($V_{e,n-1} - 2V_{e,n} + V_{e,n+1}$) and not its magnitude that is important for the excitation of nerve fibers.

2.1.3 Volume Conductor Model

In paper I, an inhomogeneous volume conductor model was used to simulate nerve fibers positioned in a nerve that was surrounded by perineurium, connective tissue, a cuff electrode and muscle fibers (see Figure 3). The nerve had a diameter of 1.4mm and the perineurium a thickness of 50μm, and it was enclosed by a cuff electrode. This electrode has a length of 8mm and an inner and outer diameter of 2mm and 3mm, respectively. The cuff electrode had three electrode contacts (configuration: anode, cathode, anode). These contacts were placed with the cathode in the center of the cuff electrode and the two anodes were symmetrically placed 3mm from the center cathode. The cuff electrode was surrounded by connective tissue that also filled the gap between the inner wall of the cuff electrode and the nerve bundle. The connective tissue filled an area of 12.8mm x 4.9mm (L x W) around the center of the cuff electrode. The rest of the volume conductor model was filled with muscle, except for a boundary layer with a thickness of 1mm. The nerve fibers all had their center node (node 0) positioned directly under the cathode.
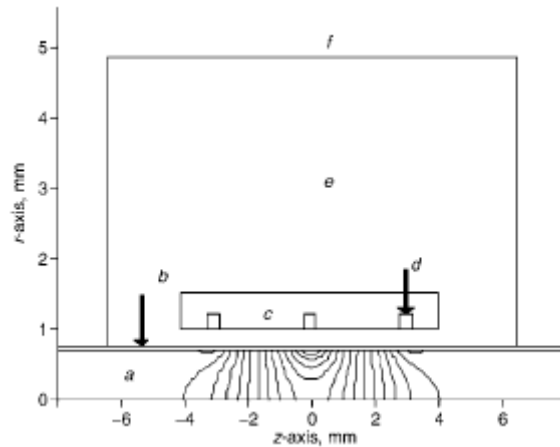
Figure 3: An illustration of the 2-D volume conductor model of a mono-fascicular nerve bundle surrounded by perineurium, connective tissue and a cuff electrode. The nerve bundle had a diameter of 1.4mm; the width of the perineurium was 50μm, and the inner and outer diameter of the cuff was 2mm and 3mm, respectively. The connective tissue was surrounded muscle tissue and a 1mm in width boundary layer that was a combined representation of distant tissue. The compartments are labeled: 1) Nerve bundle, 2) perineurium, 3) cuff, 4) electrode contacts, 5) connective tissue, 6) muscle, and 7) boundary layer (not shown). The contour lines within the nerve bundle are for an electrical stimulation of -100μA. The contour lines have a spacing of 10mV.

2.2 Rectangular prepulses (paper II)

2.2.1 Background

There is little consensus on the duration of rectangular prepulse most efficient for a selective activation of small and distant nerve fibers. Short prepulses (0.5ms to 10ms in duration) have been used for selective activation of distant nerve fibers (41;75), while prepulses used for selective activation of small nerve fibers have been an order of a magnitude longer (900ms in duration) (105).

The effect of a prepulse can be increased by increasing its intensity and partly by increasing its duration (41). However, the intensity is limited by the excitation threshold for the prepulses itself, since the selective stimulation will be lost if the prepulse is super-threshold and activates large nerve fibers. The study of Bolhuis et al. (2001) on selective activation of small nerve fibers used prepulses of 900ms in duration, while the study of Grill and Mortimer (1997) used prepulses of 0.5ms in duration. Furthermore, in modeling results on sub-threshold prepulses have shown that it has little effect to increase the duration of the prepulse to more than ~1ms, since at that time sodium channel inactivation is virtually complete (41). However, sodium channel inactivation is not the only underlying biophysical mechanism for sub-threshold prepulses. Experimental results have shown that also potassium channel activation play a significant role in accommodation to prepulses/conditioning current (3).

The weak prepulses of long duration used in the study of Bolhuis et al. (2001) was observed to selectively recruit slow muscle units, but, no studies have compared short vs. long prepulses with the same experimental paradigm. Consequently, it is an unresolved question, whether a short or long prepulse are more optimal for selective activation of small nerve fibers.

2.2.2 Methods for studying recruitment order with rectangular prepulses

Experiments were performed on six male Sprague-Dawley rats (weight: 316 − 355g). Two compound nerve action potential (CNAP) signals were recorded from the sciatic nerve, and the CNAP responses were evoked by electrical stimulation with a needle electrode of the sural nerve in the ankle (see Figure 4, for an illustration of the experimental setup).

The nerve conduction velocity (NCV) was used to quantify the change in recruitment order with rectangular prepulses, and it was estimated based on the conduction time of the CNAP signal and distance between the two hook electrodes. Two-channel recordings (conduction time) were used instead of single-channel recordings (latency) for estimating the NCV. This was due to inherent problems in estimating NCV based on the latency of a response, as the latency is determined both by the true conduction time between the stimulating and recording electrode but also by the time of activation for

the electrical stimulus (31). The time of activation is the time from the onset of a stimulus to the time when an action potential is generated, and it is mainly determined by the passive charging of the axon up to the point where the inward current becomes regenerative (31). However, since a sub-threshold prepulse depolarizes the axons it is very likely to affect the time of activation and for this reason a change in latency would therefore not necessarily imply a change in recruitment order.

The effect of 1ms, 10ms, and 100ms rectangular prepulses on the recruitment order were assessed by comparing the NCV with these prepulses with the NCV for the rectangular pulse without prepulses. The intensity of the prepulses was set to 90% of their excitation thresholds. The rectangular stimulus had a duration of 0.2ms and an intensity of 110% of its excitation threshold. The excitation thresholds of the stimulus pulses were determined just prior to it being applied with prepulses or alone. The NCV for the stimulus pulse alone was determined at the beginning of the experiment and again at the end as a control of the stability of the experimental preparation. Between these the effect of the 1ms, 10ms, 100ms prepulses were assessed, and the sequence of the prepulses was pseudo-random (Latin-squares) across the experiments.
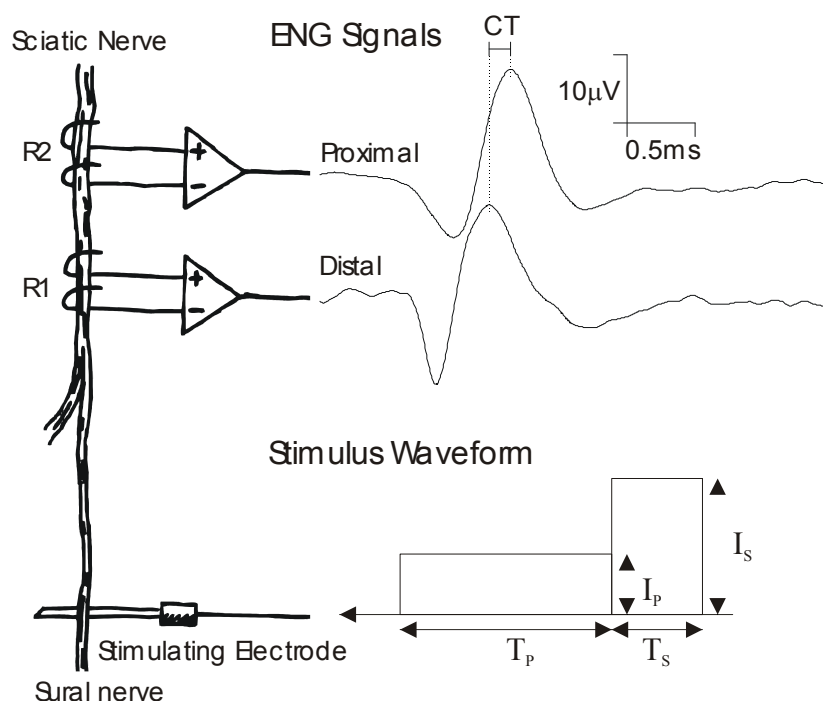
Figure 4: Illustration of the experimental setup; the sural nerve was stimulated with a needle electrode. The stimuli were defined by four parameters, the duration and intensity of the prepulse (T_P and I_P) and of the subsequent rectangular pulse (T_S and I_S). Responses were recorded from the sciatic nerve with two hook electrodes, and the conduction time (CT) was identified from the peak latencies of the two CNAP signals. The nerve conduction velocities were estimated based on the conduction time and distance between the hook electrodes.

15

2.3   Ramp prepulses (Paper III)

2.3.1   Background

Paper III, was based on Hill's theory of accommodation (48) that lead to a hypothesis; that a greater change in the recruitment order of motor neurons is possible with ramp prepulses than with rectangular prepulses. According to the modeling studies on sub-threshold prepulses, the efficacy of prepulses depends on the level of sodium channel inactivation that it induces (41). The level of sodium channel inactivation can be increased by increasing prepulse duration and intensity. However, there are limits on both the intensity and duration of rectangular prepulses. Modeling studies suggests that it has little effect to increase the duration of a prepulse to more than ~1ms, since at that time sodium channel inactivation is virtually complete (41). The intensity of a rectangular prepulse cannot exceed its excitation threshold, since it will then activate large nerve fibers or nerve fibers close to the electrode. Based on Hill's theory of accommodation (48) the limit on prepulse intensity may be removed by using ramp prepulses instead of rectangular prepulses. Hills's theory of accommodation (48) and the model described in section 2.1 Exponentially rising waveforms (personal observation), predicts the existence of critical slopes for ramp pulses (i.e. that a ramp pulses will fail to excite a nerve fiber if its slope is below the critical slope of the nerve fiber). According to this theory, the intensity of a ramp prepulse can be set to any arbitrary value if the slope of the prepulse is kept below the critical slope of the nerve to be stimulated.

There are contradictionary assumptions in the studies on prepulses vs. the studies on threshold electrotonus. Threshold electrotonus has been found to closely resemble electrotonic changes in the membrane potential of a single nerve fiber. Threshold electrotonus, however, is usually obtained from compound nerve action potentials (55) or compound muscle action potentials (54) and not from single neuron recordings. In threshold electrotonus, it is assumed that the conditioning current changes the thresholds of all nerve fibers with a constant factor (54) (indifferent accommodation). This assumption is necessary for threshold electrotonus to reflect the electrotonic changes in single nerve fibers, because without it different nerve fibers would determine the threshold for different delays between the test stimulus and the conditioning current. Sub-threshold prepulses are based on the direct opposite hypothesis that sub-threshold prepulses (conditioning current) do not change the threshold of different nerve fibers with a constant factor (differential accommodation). Instead, it is assumed to produce greater changes in large nerve fibers and in nerve fibers close to the electrode than in small and more distant nerve fibers. Consequently, this differential accommodation to prepulses/conditioning current may be the source of an error in threshold electrotonus.

2.3.2 Methods for studying differential accommodation

In paper III, differential accommodation was studied by recording stimulus-response (SR) curves for rectangular test stimuli alone and with ramp prepulses of 100ms and 500ms in duration. The responses were recorded from the abductor pollicis brevis (APB) muscle and they were elicited by electrical stimuli delivered with surface electrodes to the median nerve at the wrist. An example of a SR curve is shown in Figure 5.
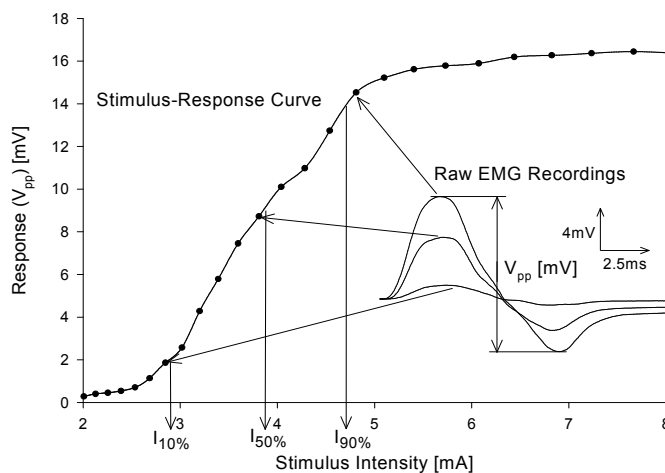

Figure 5: An example of a SR curve with indication of the $I_{10\%}$ and $I_{90\%}$ thresholds. In the example, the stimulus intensity of a 1.0ms rectangular pulse is increased in 6% steps from a sub-threshold value (~2mA) to a super-maximal value (~8mA). The insert shows the compound muscle action potentials for three different stimulus intensities (close to the 10%, 50%, and 90% thresholds).

SR curves are recorded as a part of the threshold tracking protocols for clinical evaluation of motor nerves (54) and sensory nerves (55) and the method for obtaining SR curves was taken from these protocols. The SR curves were quantified by estimation of the thresholds for a response of 10% and 90% of the supra-maximal response; these thresholds are referred to as the 10% threshold and 90% threshold, respectively.

Differential accommodation was assessed by calculating the change in the 10% and 90% thresholds with ramp prepulses from their value without ramp prepulses. If the ramp prepulses changes, the threshold of all nerve fibers with a constant factor (i.e. indifferent accommodation) then the same change should be observed for the 10% and 90% thresholds. Differential accommodation was assessed for 100ms and 500ms ramp prepulses set to 20%, 40%, 60%, and 80% of their respective excitation thresholds. For that assessment, the duration of the rectangular test stimulus was held constant (1ms). The influence of the duration of the test stimulus on differential accommodation was assessed by recording SR curves for 100ms and 500ms ramp prepulses set to 80% of their excitation thresholds and with test stimulus durations of 0.2ms, 0.3ms, 0.5ms, 1.0ms, and 2.0ms.

17

2.3.3 Methods for studying recruitment order with ramp prepulses

The existence of differential accommodation is a prerequisite for selective electrical stimulation with sub-threshold prepulses; however, its existence does not demonstrate that selective electrical stimulation is possible. Two separate methods were used in paper III, to study whether ramp prepulses may selectively activate: a) small nerve fibers and b) distant nerve fibers.

2.3.3.1 Recruitment order with respect to nerve fiber diameter

Nerve conduction velocity (NCV) testing was used to study the recruitment order of rectangular test stimuli with and without ramp prepulses. The NCVs were obtained from the responses of the APB muscle to stimulation of the median nerve at the wrist and elbow. The NCV was determined for test stimuli (intensity: 10% threshold, and 90% threshold) with and without 500ms ramp prepulses set to 80% of their excitation thresholds. The NCV with test stimuli set to their 90% threshold was primarily determined as a control of the recruitment order of the test stimulus. As discussed in the introduction there is experimental evidence for an orderly recruitment order of motor neurons with rectangular stimuli, which is in disagreement with the established theory on electrical stimulation. Consequently, in the study of the recruitment order of motor neurons with ramp prepulses it is not only a question of whether the ramp prepulses can change the recruitment order but also whether it is required (i.e. is motor neurons already orderly recruited by rectangular stimuli, even without ramp prepulses).

2.3.3.2 Recruitment order with respect to nerve fiber position

The excitation thresholds of the APB muscle and the flexor carpi radialis (FCR) muscle were used to assess the recruitment order of test stimuli with ramp prepulses. The excitation threshold for ramp pulses was estimated for prepulse of 1.0, 12.5, 25, 50, 75, 100, 200ms in duration, and these thresholds were normalized with the rheobase. The rheobase was estimated with the use of Weiss' law, by determining the excitation threshold for rectangular stimuli of 0.2ms and 1.0ms in duration (16). The excitation thresholds for the ramp pulses were used for ramp prepulses set to 80% the excitation threshold of the corresponding ramp pulse, and with this prepulse the excitation thresholds for the APB and FCR muscles were determined. Two measures were used to assess the degree of the change in the recruitment order of motor neurons with respect to their distance to the stimulating electrode:

a) Reversals in the recruitment order of the two muscles
b) Differences in the threshold change of the two muscles

2.4 Breakdown of accommodation (Paper IV)

2.4.1 Background

The study on breakdown of accommodation (paper IV) was motivated by experimental observations (paper III) that are in disagreement with Hill's theory of accommodation (48). Paper III was based on the hypothesis that ramp prepulses would be better than rectangular prepulses for selective electrical stimulation. This hypothesis was based on Hill's theory of accommodation and experimental observations (64) that predict the existence of a critical slope for excitation with ramp pulses (i.e. that the slope of the ramp has to exceed a critical slope, otherwise it will fail to excite nerve fibers regardless of its intensity). Consequently, with a critical slope there is no limit for the intensity of ramp prepulses if they are sufficiently long, while, the excitation threshold of a rectangular prepulse decrease towards the rheobase with an increase in prepulse duration. In paper III, a critical slope was not observed for ramp prepulses, which instead where found to have breakdown of accommodation (i.e. the opposite of a critical slope, that nerve fibers are excited at a near constant intensity for ramp pulses of long duration). This is in agreement with previous studies on nerve fibers under normal physiological conditions (11;62). The group of Baker and Bostock (1989) has found that Hill's theory of accommodation is only applicable to depolarized axons, such as axons in ischaemic conditions (2). However, it is not known what biophysical mechanism is responsible for the loss of breakdown of accommodation in depolarized axons or how it can be simulated with computer models of nerve fibers.

In paper IV, it is hypothesized that persistent sodium channels (channels with no inactivation) are the underlying mechanism for Breakdown of Accommodation, that these channels creates a "threshold region" of membrane depolarization that cannot be exceeded without the generation of an action potential. Persistent and late (channels with slow inactivation) sodium channels has been found in large dorsal ganglion neurons (5), and it has been found that these channels are necessary for modeling latent addition (20). The modeling study (20), suggests that persistent sodium channels are present in both sensory and motor neurons and that they have fast activation kinetics that may facilitate action potential generation. The hypothesis of persistent sodium channels as the underlying mechanism for break down of accommodation was studied both with existing models for rabbit, rat, and human nerve fibers and with a new model for human nerve fibers, which as opposed to the existing models included persistent sodium channels.

2.4.2 Existing Models

Three existing models for space-clamped rabbit (26), rat (90), and human (91) nerve fibers were analyzed with respect to their ability to reproduce breakdown of accommodation. The models for rabbit and rat nerve fibers were implemented as they appear in (78). The model for human nerve fibers was

scaled to a temperature of 37°C with the methods described in Schwarz et al. (1995) (91). For the model of rabbit and rat nerve fibers the data for a temperature of 37°C was used.

2.4.3   The New Model

2.4.3.1   Morphology

Myelinated nerve fibers, such as motor neurons, display a high degree of structural organization. They are composed of an axon and associated Schwann cells. The motor axon arises from the axon hillock at the soma (cell body) and traverses the peripheral nerve until it branches and terminates on the muscle fibers it innervates (see Figure 6).

Geometrical parameters

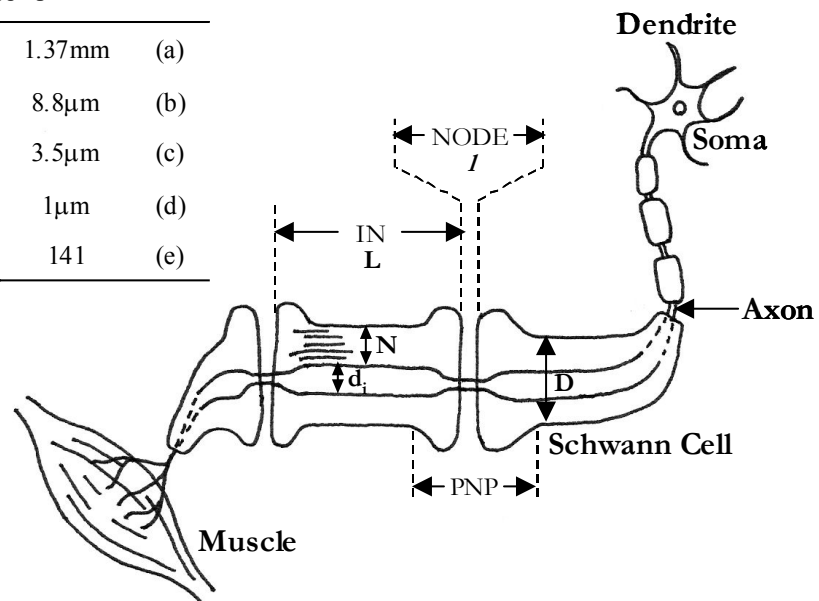|		
Inter-nodal length (L)	1.37mm	(a)
Inter-nodal diameter (d_i)	8.8µm	(b)
Nodal diameter (d_n)	3.5µm	(c)
Nodal length (l)	1µm	(d)
No. of myelin lamella (N)	141	(e)

Figure 6: Illustration of a motor neuron of diameter (D) of 14µm, which arises in the CNS were its cell body (soma) is located in the ventral horn of the spinal cord and it terminates on muscle fibers in the periphery. The enlarged portion illustrates the morphology of the motor neuron: NODE) node of Ranvier, IN) Internode, PNP) paranode-node-paranode region. References: a) Nilsson and Berthold (1988) (71), b and e) Berthold et al. (1983) (12), c) Rydmark (1981) (84), and d) Rydmark and Berthold (1983) (85).

Along the course of the axon, Schwann cells are longitudinally arranged, with myelin lamella tightly wrapped around the axon. The place where the Schwann cells meet are called nodes of Ranvier (node), which are constricted segments of the axon not covered with myelin lamella. The parts of the axon between the nodes of Ranvier are referred to as internodes (IN). The internodes can be divided into three parts; the stereotype internodal (STIN) region, proximal and distal end regions (also referred to as paranodes (PN)), and myelin sheath attachment (MYSA) regions. The transition from the STIN region to the paranode is marked by an increase in the volume of the Schwann cell and by an irregular constriction of the axon. In the paranode region, the Schwann cell also becomes rich in mitochondria and there are irregularities in the myelin lamella. The transition from paranodes to nodes of Ranvier is marked by the MYSA segments, where the myelin lamellas terminates and are attached to the axon.

The space between the axon and the inner cell membrane of the Schwann cell (adaxonal membrane) is a narrow gap (1 – 30nm), which is referred to as the periaxonal space. The reader is referred to Berthold and Rydmark (1995) (13) for a more extensive review on the morphology of peripheral nerve fibers.

The model was based on the morphology of a nerve fiber with diameter (D) of 14μm. The axon at the internode and node of Ranvier was described as cylinders with constant internodal diameter (d_i), and nodal diameter (d_n). The membranes of the myelin lamella (two membranes per lamella) were regularly spaced from the adaxonal membrane to the outer cell membrane of the Schwann cell. The width of the periaxonal space was assumed negligible and set to zero. For comparison, the width of the periaxonal space is estimated to be between 1-2nm to 30nm (13) (depending on the preparatory procedure) and the width the Schwann was 5200nm (12).

2.4.3.2   Electrical Equivalent Circuit

The model had several parameters, for which there are limited or no experimental data. For that reason it was considered essential that the model would not only reproduce breakdown of accommodation (62), but would also reproduce multiple sets of independent experimental data related to different aspects of accommodation and action potential generation. These experimental data were; threshold electrotonus (109), recovery cycle (54), and latent addition (72) (see paper IV for a description of these experimental data). At the same time, the model was chosen so it would be the simplest model that could still reproduce these sets of experiments data.
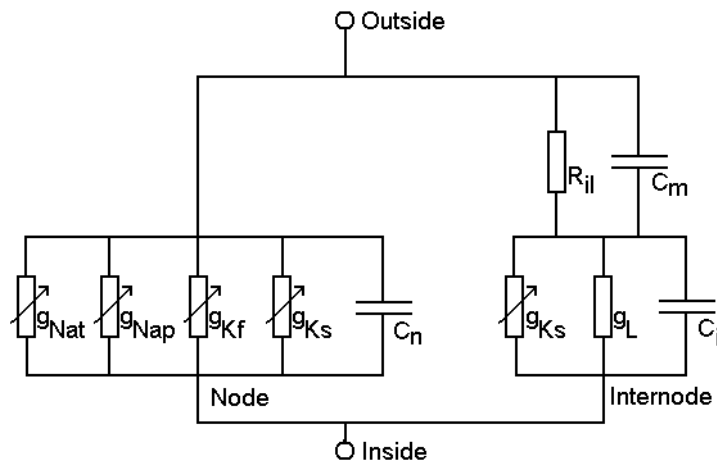

Figure 7: Equivalent circuit for a motor neuron space-clamped motor neuron. The model consisted of a node and an internode. Both the node and the internode contained non-linear current sources, which were calculated from equilibrium potentials and conductances. Channel types and maximum ionic conductances: node, transient sodium (Na$_t$, 276nS), persistent sodium (Na$_p$, 7.1nS), fast potassium (K$_f$, 4.1nS), and slow potassium (K$_s$, 17.4nS); internode, slow potassium (Ks, 87.1nS) and leak conductance (L, 1.7nS). The linear parameters of the model: C$_n$, nodal capacity (0.22pF), C$_i$, internodal capacity (379pF), C$_m$, capacity of the myelin sheath (0.17pF), and R$_{il}$, internodal leak resistance (41MΩ).

A simple one-compartment model for a space-clamped motor axons cannot explain threshold electrotonus and recovery cycles as it does not have a representation of the internodes. The passive

charging of the inter-nodal axolemma is important for the S1 phase in threshold electrotonus (2;3) and the depolarizing after-potentials in the recovery cycle (9). Furthermore, the S2 phase of electrotonus is dependent on internodal slow potassium channels (3). A two-compartment model, with a representation of the node of Ranvier and the internode was therefore chosen. The electrical equivalent circuit of the model was based on models that previously have been used for studying electrotonus and latent addition (17;18;20) (see Figure 7).

The nodal (C_n), internodal (C_i), and myelin (C_m) capacitances were calculated based on the geometrical parameters described in the previous section and experimentally estimated capacitances per square micrometer (node: $2\mu F/m^2$ (37), internode: $1\mu F/m^2$ (21), and myelin lamella: $0.1\mu F/m^2$ (98)). The inter-nodal leak resistance (R_{il}) was set by trial-and-error to a value that allowed reproduction of the experimental data used for validating the model. This approach was used, as there is little experimental data on the inter-nodal leak resistance. Only modeling data exists for the periaxonal resistivity (43) and modeling studies have shown that the longitudinal conductance of the myelin sheaths has to be taken into account in determining the inter-nodal leak resistance (93). The longitudinally conductance of the myelin sheaths implies that the model either needs a representation of all the myelin sheaths or an equivalent value has to estimated for the inter-nodal leak resistance. In paper IV, the last approach was employed as the model otherwise would be very extensive (93), and the unknown resistivity of the periaxonal space would prevent an experimental determined value even with a more extensive model.

2.4.3.3   Ionic Currents

Five distinct types of potassium channels have been identified in myelinated nerve fibers (80), which are likely to be responsible for the fast paranodal (32;36;60;104), slow nodal (91) and slow internodal (3;58;86) potassium currents. However, the channel kinetics is only known for a subset of these five potassium channels (80). Slow potassium channels were included in both the node of Ranvier and internode, but since the model had no representation of the paranode, it was not possible to include fast potassium channels in the paranode. Instead, the same approach as Wesselink et al. (1999) (108) was used and the fast potassium channels were included in the node of Ranvier as an approximation to being located in the paranode. Besides the classical transient sodium channel (26;37;49;91) three persistent and late sodium currents have been identified in mammalian nerve fibers (6). Even though three distinct persistent and late sodium currents have been identified, only the Nav(1.6) sodium channel is found in the node of Ranvier (25) and the kinetics these currents have not been described in sufficient detail to allow modeling of these currents. Instead, the three persistent and late sodium currents were represented by a single stereotypical persistent sodium channel. The kinetics of this stereotypical persistent sodium

channel was based on the work of Bostock and Rothwell (1997) (20) on the influence of persistent sodium current on latent addition, and it was included in the node of Ranvier.

	Conductance (pS)	Density (channels/μm^2)
Internode:		
g_{Ks}	8	0.3
Node:		
g_{Ks}	8	100
g_{Nat}	13	975
g_{Nap}	13	25

Table 1: Single channel conductances (89) and channel densities (slow potassium (87) and sodium (89)). The percent of sodium channels (2.5%) that would be persistent was set by trial-and-error (see text).

The transient sodium channel was included in the node of Ranvier; however, following the work of Bostock and Rothwell (1997) (20) the transient sodium channels were omitted from the internode for simplicity. The ionic currents were modeled as being generated by membrane conductances (see Figure 6), and the maximum conductances for the sodium and slow potassium channels were found from single channel conductances and channels densities (see Table 1).

The channel density of the slow potassium channels in the internode and the percentage of the total number of sodium channels (1000channels/μm^2 (89)) that would be persistent was set by trial-and-error to a value that allowed the model to reproduce experimental data. The conductance of the fast potassium current was set from an estimate of the membrane area in work of Schwarz et al. (1995) (91), which was based on the nodal capacitance in experimental data and the nodal capacitance per square micrometer (37).

2.4.3.4 Membrane kinetics

Except for the slow potassium kinetics, the membrane kinetics was taken unmodified from the human data obtained by Schwarz et al. (1995) (91). The rate constants were scaled to a body-temperature of 37°C, by appropriate Q_{10} factors (91). However, in order to allow the model to reproduce the S2 phase of threshold electrotonus it was necessary to change the slow potassium kinetics, which were changed in order to slow channel activation and to decrease the number of open channels at the resting potentials for the internode and node of Ranvier.

2.4.4 Validation of the new model

Four sets of experimental data were used for validating the model; threshold electrotonus (109), recovery cycle (54), latent addition (72), and accommodation curve (slope, and presence of breakdown of accommodation) (62). To allow the model to reproduce these experimental data, the following parameters were adjusted:

a) Inter-nodal leak resistance (R_{il})

b) Density of internodal slow potassium channels

c) Number of persistent sodium channels (set as a percentage of the total number of sodium channels)

d) Nodal resting potential

e) Kinetics of the slow potassium channel.

Please refer to paper IV or reviews (19;23) for a description of the methods used for validating the model.

3 Exponentially rising waveforms (Paper I)

In paper I, selective activation of small (8μm) motor neurons was observed with exponentially rising waveforms. An example of a selective activation of a small motor neuron with an exponentially rising waveform of 2ms in duration and time-constant of 1ms is shown in Figure 8.
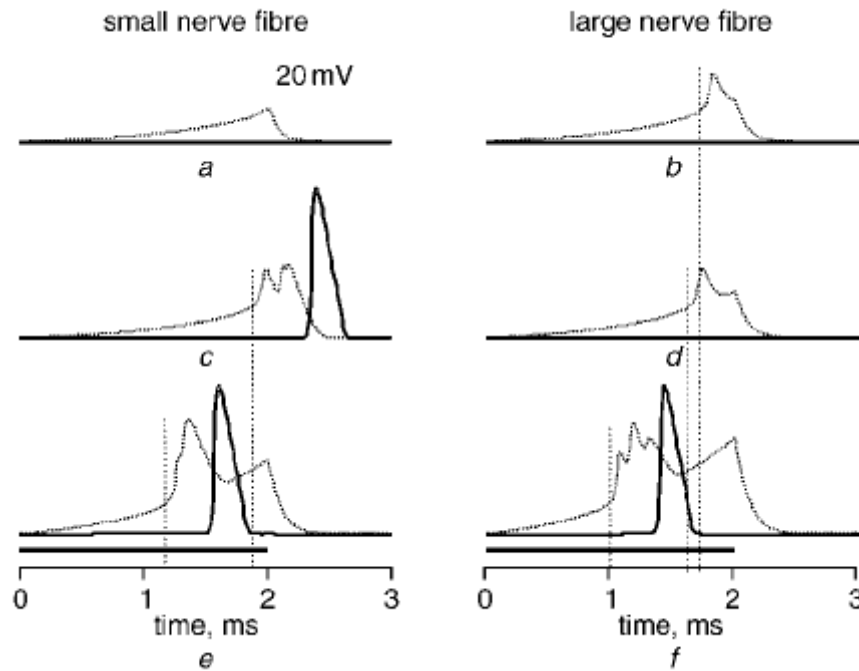

Figure 8: Responses of the membrane potentials of small α-motor neurons (8.0μm) and large α-motor neurons (15.5μm) to exponentially rising stimuli. The stimuli had a duration of 2ms (shown by the thick line in E and F), time-constant of 1ms, and three different intensities: A, B) 90% of the current threshold of the small α-motor neurons (47.5μA), C, D) the current threshold of the small α-motor neurons (52.8μA), and E, F) the current threshold of the large α-motor neurons (125.1μA). The nerve fibers were positioned at the edge of the nerve bundle and with their central node directly under the stimulating cathode (bold line: central node, thin line: outside the cuff). The figure is taken from paper I.

Initially, with current equal to 90% of the threshold current of the small α-motor neuron, both the small (8μm) and large (15.5μm) α-motor neuron had a local excitation. However, even though the local excitation was markedly larger in the large α-motor neuron it failed to generate a propagating action potential. Increasing the current to the threshold current of the small α-motor neuron displaced the local excitation of the large α-motor neuron forward in time, whereas it did not create a propagating action potential as in the small α-motor neuron. Finally, the large α-motor neuron fired a propagating action potential with a current 2.36 times the current threshold of the small α-motor neuron. Thus, for this exponentially rising waveform the recruitment order was reversed as compared to the recruitment order of rectangular pulses.

Unlike sub-threshold prepulses, differences in sodium channel inactivation or other membrane properties cannot explain the selective activation of small nerve fibers with exponentially rising waveforms. This conclusion is based on a simulation that demonstrated that the membrane potential of a small and large nerve fiber could be matched so they had identical responses before a local excitation occurred.
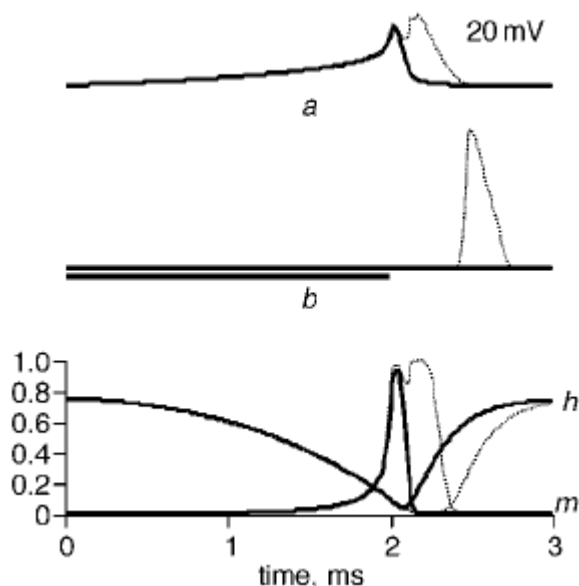

Figure 9: Membrane potential (A and B) and sodium channel inactivation (C) for a large (15.5μm) α-motor neuron (thin lines) and a small (8μm) α-motor neuron (bold lines), during an exponentially rising stimulus (duration: 2.0ms, time-constant: 1.0ms). The intensity of the stimulus is set to the current threshold of the small α-motor neuron. The membrane potentials are shown at two positions: A) the central node, and B) node number three, which is outside the cuff (location in z-axis: -13.6mm and –12.4mm for small and large α-motor neurons, respectively). The figure is taken from paper I.

However, even though the sub-threshold responses are identical, the local excitation only generates a propagating action potential in the small nerve fiber, while action potential propagation fails in the large nerve fiber (see Figure 9). This is a consequence of a model that have identical parameters for large and small nerve fibers and where the differences between nerve fibers of different diameters only can be accounted for in terms of differences in the extra-cellular potential (see section 2.1.2 Nerve Fiber Model). Instead, the different reaction of large and small motor neurons could be explained with differences in the membrane potentials, a difference that was described in terms of a "deactivating function".

3.1 Deactivating Function

Disregarding sodium channel kinetics, the membrane potential is depolarized by the difference in extra-cellular potential along the nerve fiber ($V_{e,n-1} - 2V_{e,n} + V_{e,n+1}$) (see page 12), which in the following will be referred to as the activating function (it is proportional to the activating function ($V_{e,n-1} - 2V_{e,n} + V_{e,n+1}$)/$x^2$ defined by Rattay (76;77)). Near a cathode, the activating function leads to membrane

26

depolarization, which is largest directly under the cathode (see Figure 10A). Because of the positive relation between nerve fiber diameter and internodal distance, membrane depolarization is larger in large than in small nerve fibers. However, the same relation also implies that there is a larger difference in membrane potential between adjacent nodes in large nerve fibers than in small nerve fibers (see Figure 10A). Consequently, the first term in the cable equation $(V_{n-1} - 2V_n + V_{n+1})$ (see page 12) for the nerve fiber model is also greater in large nerve fibers than in small nerve fibers, but unlike the activating function, this term is inhibitory for action potential generation (see Figure 10B). The term $(V_{n-1} - 2V_n + V_{n+1})$ will be referred to as the deactivating function.
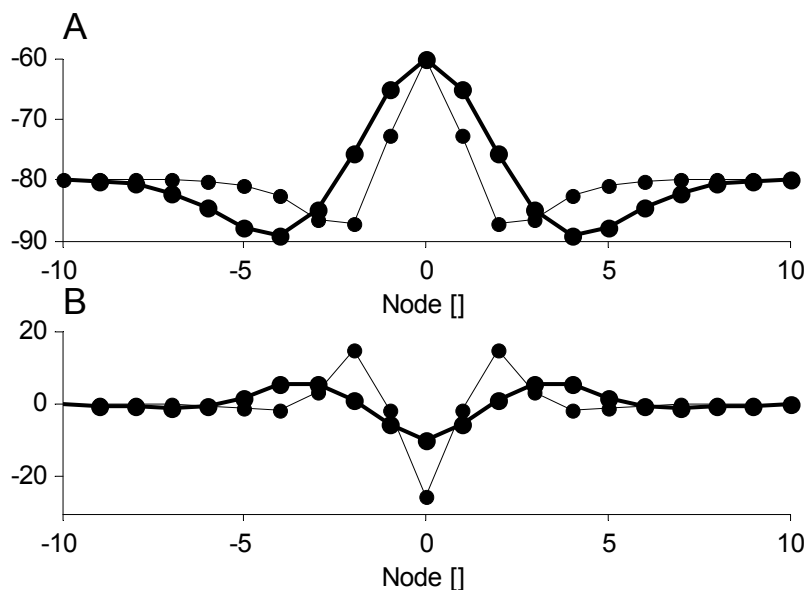

Figure 10: The membrane potential (A) and the deactivating function $(V_{n-1} - 2V_n + V_{n+1})$ (B) of a large (thin line) and small (bold line) nerve fiber. Linear models were used in the simulation, where the sodium channel conductance was a constant set to its value at the resting potential. The stimulation intensities were matched so the membrane depolarization induced in the center node (node 0) would be the same for the large and small nerve fiber. The figure is taken from paper I.

For rectangular pulses, large nerve fibers are recruited before smaller nerve fibers despite the differences in the deactivation functions. This is a consequence of the much larger difference between the activating functions of large and small nerve fibers. However, when the amplitude of the action potential is reduced due to sodium channel inactivation, the propagation of the action potential will eventually fail. In paper I, it was found that due to the differences in the deactivation function for large and smaller nerve fibers, it would fail in large nerve fibers before it failed in smaller nerve fibers. Consequently, the deactivating function was found to form the mechanism by which exponentially rising waveforms activate small before large nerve fibers. Furthermore, it provides a framework by which optimal electrode geometries can be designed for selective electrical stimulation using stimulation methods that relies on accommodation. This optimal electrode design would be a design that maximizes the difference in the deactivating function between small and large nerve fibers.

In paper I, a rectilinear relationship between nerve fiber diameter and internodal length was assumed, which resulted in a model with constant parameters independent of nerve fiber diameter. However, this rectilinear relationship is only an approximation. Experimental data has demonstrated that the relationship between nerve fiber diameter and internodal length is logarithmic rather than linear (i.e. a greater difference in inter-nodal length is observed for small nerve fibers than for large nerve fibers) (10;71). With a logarithmic relationship, the deactivating functions for large and small nerve fibers are not directly comparable, but it will not change the relation; that the deactivating function increases with an increase in nerve fiber diameter, this relation is only dependent on a positive correlation between diameter and internodal distance. Our group has in a preliminary study (46), demonstrated that selective electrical stimulation of small nerve fibers also is possible with the model of Wesselink et al. (1999) (108). The model of Wesselink et al. (1999) has a non-linear logarithmic relationship between diameter and internodal distance, and this demonstrate that in theory the effect of exponentially rising waveforms is not dependent on a rectilinear relationship.

4   Sub-threshold prepulses (Paper II and III)

4.1   Recruitment order with rectangular prepulses

In paper II, the rectangular prepulses were observed to decrease the nerve conduction velocities (NCV) of the CNAP responses (see Figure 11). The NCV with 1ms, 10ms, and 100ms rectangular prepulses decreased by 17.3 ± 5.2m/s, 17.4 ± 3.1m/s, and 13.4 ± 4.2m/s, respectively. The observed decreases in NCVs for 1ms and 10ms prepulses suggests that rectangular prepulses may be effective for selective activation of small motor neurons, as they are larger than the range of NCVs from 8/ms to 17m/s (mean: 12m/s) of motor neurons in the ulnar nerve (27).

The results of paper II do not support the hypothesis of van Bolhuis et al. (2001) (105) that by increasing the duration of weak prepulses they are just as effective as short intense prepulses. Instead, there was not observed any significant difference in NCV between prepulses of 1ms, 10ms, 100ms in duration. This observation supports the original prepulse paradigm of Grill and Mortimer (1997) (41) who used short prepulse (~1ms) with intensities close to their excitation thresholds. However, the stimulation method in paper II is different from the method of van Bolhuis et al. (2001) (105). In paper II, the longest prepulses was 100ms in duration, whereas, the prepulses in the study of van Bolhuis et al. (2001) were 1500ms in duration (stimulation pulse superimposed 900ms after the onset of the prepulse). Due to technical limitations, it was not possible to use prepulses with the same duration as in the study of van Bolhuis et al. (2001) (105). It has to be acknowledged that other mechanisms may be active with prepulses of 1500ms in duration than with 100ms. For example, activation of the sodium-potassium

pump, or pH changes in the vicinity of the electrodes, which may have increased the effect of the 1500ms prepulses. However, on the functional level there is little reason to use 1500ms prepulses when 1ms prepulses appear to be equally effective. One reason is that 1500ms prepulses do not allow stimulation frequencies of 30Hz to 50Hz, which is needed for smooth muscle contractions in functional electrical stimulation (92).
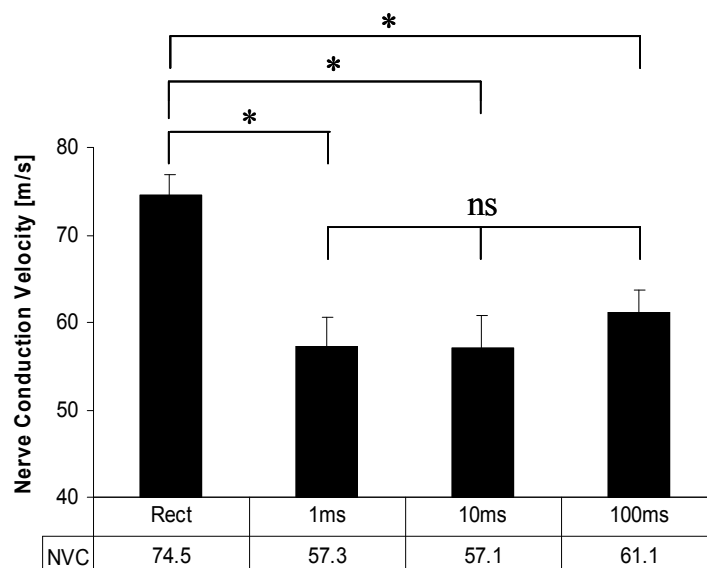

Figure 11: Nerve conduction velocities (NVC) without a prepulse (Rect) and with prepulses of 1ms, 10ms, and 100ms in duration (tukey test, * P < 0.025, ns: non-significant).

4.2 Recruitment order with ramp prepulses

In paper III, ramp prepulses were observed to change the recruitment order of motor neurons stimulated with ramp prepulses and rectangular stimulation pulses. A change in recruitment order with respect to nerve fiber diameter was observed from the reduction in the NCV of 10% responses (i.e. responses that are 10% of the supra-maximal response) with ramp prepulses compared to without ramp prepulses. With a 500ms ramp prepulse set to 80% of its excitation threshold the NCV was reduced with 4.3m/s. This suggests that rectangular pulses with ramp prepulses do not recruit the largest nerve fibers first but instead smaller nerve fibers. However, the results of paper III do not allow for an assessment of the magnitude of the change in recruitment order, whether it is large enough to completely reverse the recruitment order of motor neurons. The CV of the initial responses could not be determined as that estimate is likely to be significantly biased by the time of activation (see section 2.3.3.1 Recruitment order with respect to nerve fiber diameter).

As a control, the CV of the 10% and 90% responses with rectangular pulses alone were determined, and no significant difference was observed between them. This suggests that large nerve fibers are recruited

first by rectangular pulses; otherwise, there should be an increase in the CV from the 10% to the 90% response. The results of paper III were consequently found to be in disagreement with the studies of Thomas et al. (2002) (101) and Godfrey et al. (2002) (39) in which an orderly recruitment of motor neurons was observed with rectangular pulses.

Selective activation of small nerve fibers with surface electrodes has proven to be challenging for most previous stimulation methods. Selective recruitment of small diameter nerve fibers has been reported using anodal blocking (1;33;34;81), high frequency stimulation (8), block by direct current (38;65;88;112) and ramp pulses (63). Unfortunately, anodal blocking does not work with surface electrodes (30), and no studies have investigated the possibility for selectively recruiting small diameter motor neurons with high frequency stimulation or block by direct current using surface electrodes. High frequency stimulation appears to be ineffective with surface electrodes (personal communication, Brian Andrews). However, exponential waveforms, which are comparable to ramp pulses, have been reported by Kugelberg and Skoglund (1946) to selectively recruit small before large diameter motor neurons using surface electrodes (63). The reasons why no studies have tested this method for use in FES remain unclear. More research is required to reproduce the results of Kugelberg and Skoglund (1946) for comparing the feasibility of ramp pulses alone and ramp pulses as prepulses to rectangular stimuli.
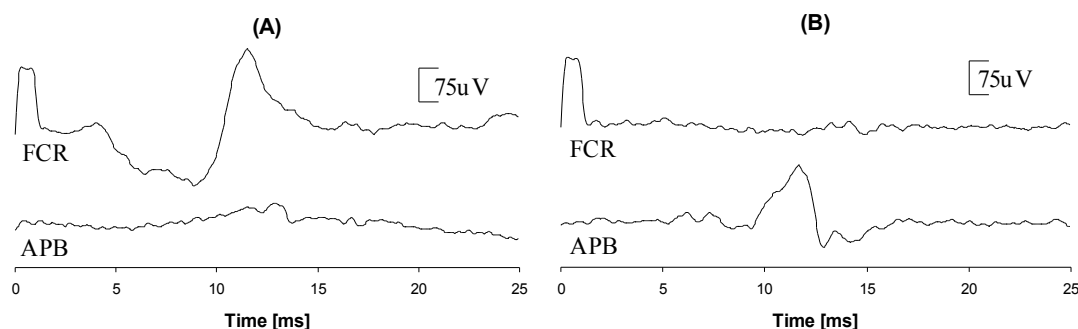

Figure 12: An example of a reversal of the recruitment order of muscle A and B. The reversal was obtained by with a 100ms ramp prepulse set to 80% of its excitation threshold for muscle A (muscle A was defined as being the muscle with the lowest threshold to rectangular stimuli). Subfigure 5A and 5B show the response to a stimulation that is just capable of evoking a response in either muscle A or B. The response of muscle A and B to the test stimulus alone is shown in subfigure 5A. In subfigure 5A, the test stimulus has an intensity of 2.27mA, and there was only recorded a CMAP from muscle A. In subfigure 5B, the test stimulus was preceded by a ramp prepulse, and the recruitment order was reversed (i.e. there was only recorded a CMAP from muscle B). In subfigure 5B, the test stimulus had an intensity of 2.16mA. The figure is taken from paper III.

In paper III, reversals of the recruitment order of the abductor pollicis brevis (APB) and flexor carpi radialis (FCR) muscles was observed with ramp prepulses (an example is shown in Figure 12). Reversals of the recruitment order of the APB and FCR muscles were observed in seven out of 13 subjects; however, these reversals were not obtained for the same duration prepulse. The highest number of reversals in the recruitment order of APB and FCR muscles for any single prepulse was obtained for the prepulse of 1ms in duration, for which there was obtained four reversals out of 13 experiments.

30

Consequently, between subjects a considerable variability in the effect of the different prepulses was seen.

A differential effect of the excitation thresholds of APB and FCR muscles was observed, where the excitation threshold of the most excitable muscle with test stimuli alone were effected more than the threshold of the least excitable muscle (see Figure 13).
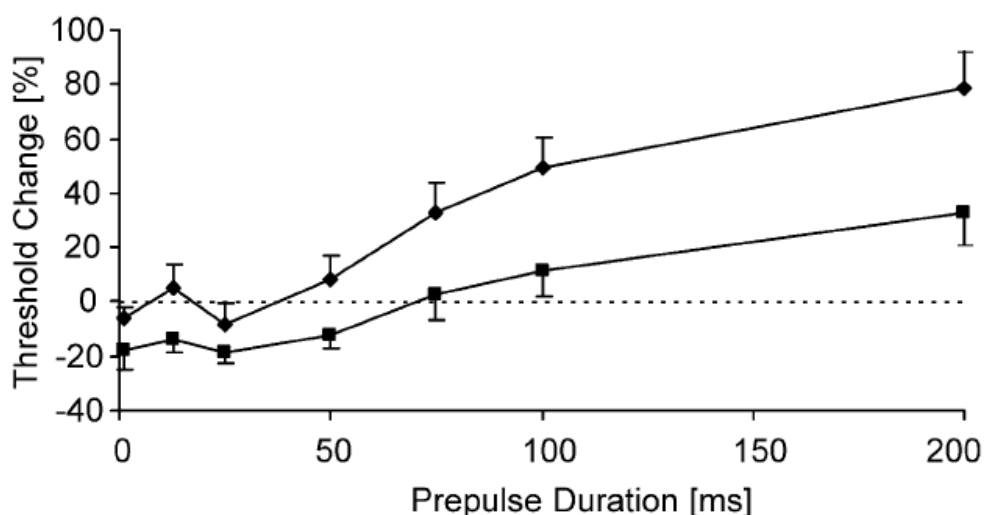

Figure 13: The change in the excitation thresholds for (♦) muscle A and (■) muscle B as a function of prepulse duration. Muscle A was defined as the most excitable muscle with rectangular stimuli alone. The threshold change was calculated from the excitation thresholds of the test stimulus alone, and was obtained for test stimuli of 1.0ms duration. The ramp prepulses was set to 80% of their respective excitation thresholds. The figure is taken from paper III.

The differential effect of the excitation thresholds of APB and FCR muscles were interpreted as evidence for a position dependent accommodation to ramp prepulses. For this interpretation, the excitation thresholds of the two muscles have to be determined by their position to the stimulating electrode and not by a difference in the diameters of the motor neurons innervating the two muscles. The FCR muscle is usually innervated by a single branch of the median nerve that arises below the anticubital fossa (94). However, even though it arises below the anticubital fossa a branch is likely to be confined to the same region of a nerve (106). As, the FCR and APB muscles are innervated by two different branches of the median nerve this suggests that their motor neurons are located in two different regions of the median nerve at the level of the anticubital fossa. Consequently, it is likely that the difference in excitation threshold of the two muscles are the result of a different position with regard to the stimulating electrode, and that the differential effect of prepulses on these thresholds is a result of position dependent accommodation.

4.3 Differential accommodation

In paper III, stimulus-response curves were used to study differential accommodation in order to assess the mutually exclusive assumptions behind sub-threshold prepulses (41) and threshold electrotonus (19;54;55) that prepulses/conditioning current either do or do not change the threshold of nerve fibers with a constant factor (indifferent accommodation vs. differential accommodation). The 10% and 90% thresholds were used to assess differential accommodation, as an observation of a different increase in the two thresholds with prepulses would be a contradiction of the assumption of indifferent accommodation to prepulses/conditioning current.
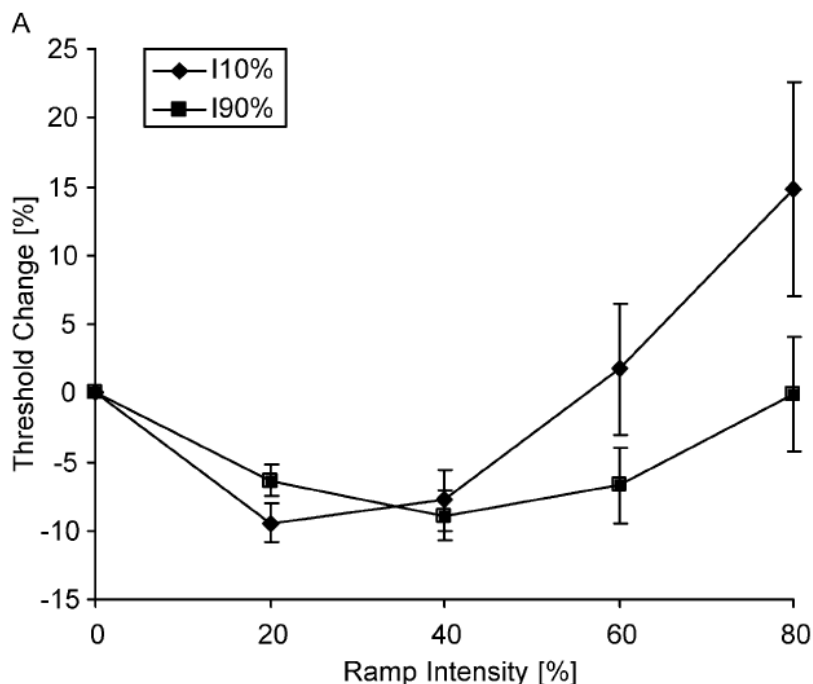

Figure 14: The change in (♦) $I_{10\%}$ and (■) $I_{90\%}$ thresholds as a function of prepulse intensity, which is shown as a percentage of its excitation threshold. The data are shown for test stimuli of 1ms duration and a prepulse duration 100ms. The figure is taken from paper III.

In paper III, the prepulses were observed to have a differential effect on the 10% and 90% thresholds. This effect was dependent on both the intensity of the prepulse and the duration of the test stimulus. Furthermore, with 100ms prepulses, the 10% and 90% thresholds were observed first to decrease and subsequently to increase when the intensity of the prepulse was increased (see Figure 14). This U-shaped function of depolarizing current has also been observed previously (59).

With regard to accommodation, paper III support the view that there is differential accommodation to prepulses/conditioning current. Consequently, this result suggests that for the technique of threshold electrotonus, both the desired response and the duration of the test stimulus should be considered before results can be compared across studies.

4.4 Accommodation to rectangular and ramp prepulses

In paper I, it was found that accommodation to prepulses cannot be accounted for by sodium inactivation alone but also the deactivating function has to be taken into account in modeling studies. Furthermore, the 10% and 90% threshold were observed to be a U-shaped function of prepulse intensity with first a decrease and a subsequent increase in threshold. The initial decrease in threshold may be explained by passive depolarization of the membrane (19;23) by the prepulse and perhaps activation of persistent sodium current. Based on paper I and III, it is suggested that the effect of prepulses may be explained by a combination of the following mechanisms: a) a decrease in threshold due to membrane depolarization (19;23) and possible persistent sodium current, and b) an increase in threshold due to sodium inactivation (41), potassium activation (3), and deactivating function (paper I). Then small nerve fibers may be selectively activated since they are depolarized less by the prepulse leading to a decrease in their thresholds, while large nerve fibers are more severely depolarized leading to an increase in their thresholds. Consequently, the effect of prepulses is suggested to be a complex interplay between both linear and non-linear mechanisms that either decreases or increases the excitation threshold.

5 Breakdown of accommodation (Paper IV)

5.1 Existing models

In paper IV, three existing models for rabbit (26), rat (90), and human (91) nerve fibers were tested for their ability to reproduce breakdown of accommodation. When nerve fibers have critical slopes (64) the accommodation curves to both exponentially rising and linearly rising currents are straight lines (48) (note: in these studies the exponentially rising current has the form: $I_S(e^{-t/\tau}-1)$). However, under normal physiological conditions the accommodation curve is not a straight line but flattens out and becomes nearly horizontal for long duration exponentially rising currents (62).

The three existing models had critical slopes to linearly rising currents (see Figure 15A) and their accommodation curves were significantly different from the accommodation curves reported in paper III (see Figure 15B) for abductor pollicis brevis and flexor carpi radialis in human subjects. The excitation thresholds of the models to linearly rising currents were all an order of magnitude higher than the thresholds recorded in human subjects, and the accommodation curves in human subjects cannot be described as simple straight lines. Consequently, significant discrepancies between the three existing models for rabbit, rat, and human nerve fibers and experimental data are evident.
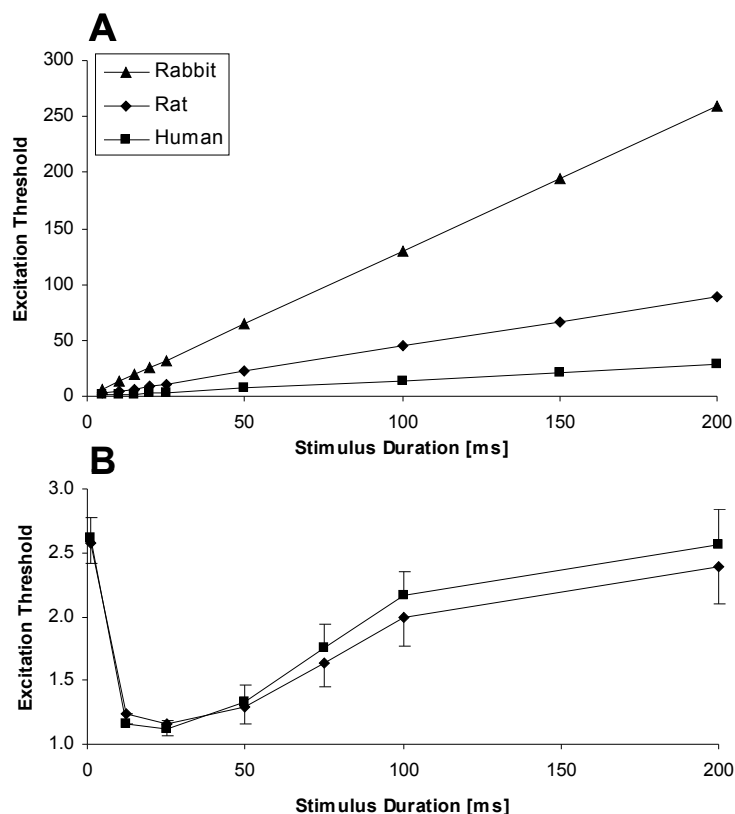
Figure 15: The accommodation curves to linearly rising current for: A) Three existing models for rabbit, rat, and human nerve fibers. B) Human subjects for (◆) abductor pollicis brevis, and (■) flexor carpi radialis (paper III).

5.2 Persistent sodium current

In paper IV, a new model of a space-clamped motor neuron (see section 2.4.3 The New Model) was used to test the hypothesis that persistent sodium current is the underlying mechanism for breakdown of accommodation and that including persistent sodium current in a model allow this phenomenon to be reproduced.

The model presented in paper IV, demonstrated that breakdown of accommodation can be reproduced when persistent sodium channels are included in the model, and that the model also could reproduce nerve properties, which are observed using the techniques of threshold electrotonus, the recovery cycle, and latent addition (see Figure 16). Furthermore, the model could only reproduce breakdown of accommodation when the persistent sodium current was activated near the resting potential and had a short time constant of activation. These predictions are in agreement with experimental observations, where the persistent and late sodium current found in large dorsal root ganglion cells was activated near the resting potential and had fast activation kinetics (5;6). This persistent sodium current is likely to be present in both large sensory and motor neurons, as they are needed for explaining latent addition in both types of neurons (20). That persistent sodium current can explain latent addition suggests that persistent sodium current can produce regenerative currents that can facilitate action potential

generation. Furthermore, persistent sodium current has been shown to amplify otherwise sub-threshold depolarization so action potentials are initiated (4). Ischaemia and hyperventilation has been shown to decrease and increase breakdown of accommodation, respectively (62). While, acidification and alkalization within physiological values have been found to decrease and increase persistent sodium current (7). The decrease and increase of breakdown of accommodation in ischaemia and hyperventilation, is consistent with the relation between persistent sodium current and acidification and alkalization. Thus, these observations support a link between persistent sodium current and breakdown of accommodation.
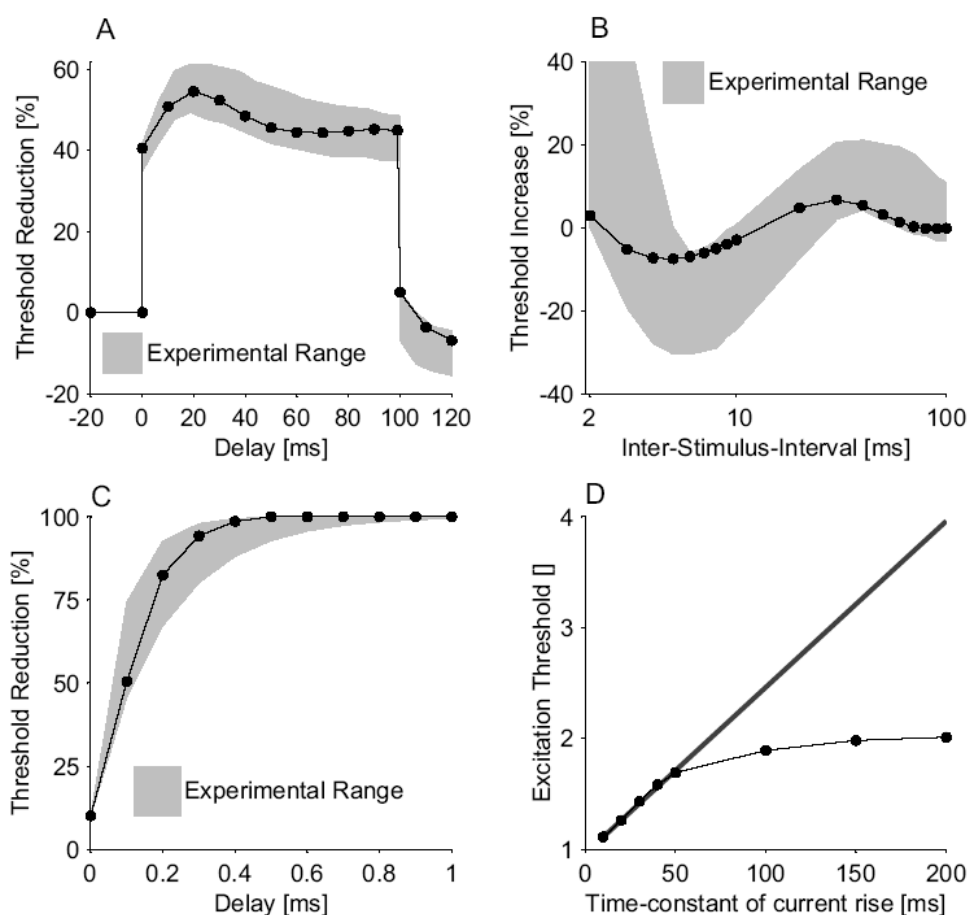

Figure 16: Comparison of the model with experimental data for: A) threshold electrotonus (109), B) recovery cycle (54), C) latent addition (72), and D) accommodation curve (62). In threshold electrotonus a sub-threshold, conditioning pulse is used to alter the threshold of a test stimulus that are delayed with respect to the onset of the conditioning pulse. In the recovery, cycle the nerve fibre is excited by a supra-threshold stimulus and the threshold of a test stimulus is determined at inter-stimulus-intervals (T_{ISI}) of 2ms to 100ms. In latent addition a short duration sub-threshold conditioning stimulus is used to alter the threshold of a test stimulus, the onset of the test stimulus is delayed with regard to the onset of the conditioning stimulus. In the accommodation curve the threshold of stimuli of the form $I_S(1-e^{-t/\tau})$ is determined, where τ is the time-constant of current rise. The figure is taken from paper IV.

5.3 Alternative explanations

Alternative explanations for breakdown of accommodation could be the gating mode of the transient sodium channels (74) or m-h overlap of their activation/inactivation kinetics (52).

The new model presented in paper IV assumes that activation and inactivation proceeds independent of each other (i.e. the formalism of Hodgkin and Huxley (1952) (49)). However, it is now known that activation and inactivation are interdependent, and that most transient sodium channels may go through an open state before entering an inactivated state (74). This gating mode of the transient sodium channel may have a synergistic role with persistent sodium current in producing breakdown of accommodation. It may be speculated that a transient channel with little inactivation before channel opening would not permit or limit a critical slope and may produce breakdown of accommodation. This may have implications for the results of paper IV. For example, the interdependence between transient sodium channel activation and inactivation is likely to change the number of persistent sodium channel that are needed for producing breakdown of accommodation.

A second explanation for breakdown of accommodation may be m-h overlap of the activation/inactivation kinetics of the transient sodium channel. For transient sodium channels, there is a region of membrane depolarization in which persistent sodium current is generated by the transient sodium channel (52). This is caused by channel activation while the membrane is still not depolarized sufficiently for all the channels to inactivate, a phenomenon that has been termed m-h overlap. A theoretical study has demonstrated that the original model of Hodgkin and Huxley of squid axons has breakdown of accommodation as a result of m-h overlap (52). In paper IV and other studies (20;66) persistent sodium channels are modeled as discrete channels, however, this does not imply that they are physically different from transient sodium channels. As previously discussed, tree discrete persistent and late sodium currents has been identified based on their inactivation kinetics (6) besides the classical transient sodium current (91), but only one sodium channel Nav(1.6) has been found in the node of Ranvier of large peripheral nerve fibers (25). This may suggest that persistent and late sodium currents are not generated by special persistent or late sodium channels, but instead by transient sodium channels that operate in a gating mode with no or slowed channel inactivation. The modeling of persistent sodium current as created by persistent sodium channels only represent the way this current is generated in the model, it cannot provide evidence for the existence of persistent sodium channels only evidence for the likelihood of a persistent sodium current that can lead to breakdown of accommodation. Consequently, this persistent sodium current may be created by m-h overlap. However, in the studies on persistent sodium current it has been argued that m-h overlap is not consistent with the observed kinetics for the persistent sodium current (5;6). Evidently, in mammalian nerve fibers, persistent sodium current is most likely not generated by m-h overlap, but the study of (52) suggests that m-h overlap may be important for persistent sodium current and breakdown of accommodation in squid axons.

5.4   Implications for threshold electrotonus

In a study of Baker and Bostock (1989), the mechanism of accommodation was observed to change from potassium channel activation to sodium channel inactivation when nerve fibers became depolarized or ischaemic (2). This change was reflected in electrotonus and threshold electrotonus; under normal physiological conditions, electrotonus and threshold electrotonus closely resemble each other (i.e. threshold is an index of membrane potential), however in ischaemic conditions, this relation is lost (2). In paper IV, it was studied whether this change in accommodation could be explained by a loss of persistent sodium current due to ischaemic acidification, as persistent sodium current decreases with a decrease in pH (7).
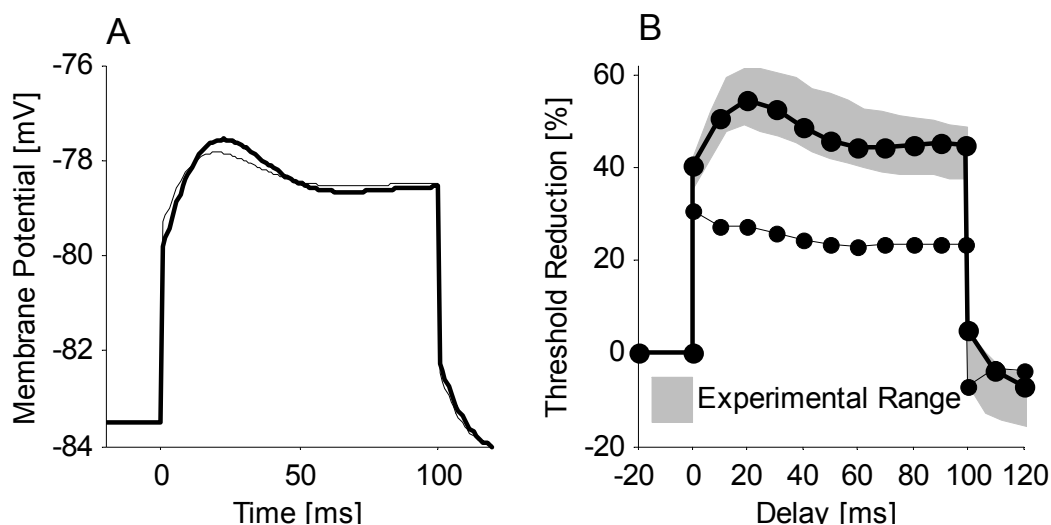

Figure 17: Electrotonus (A) and threshold electrotonus (B) of a model with persistent sodium channels (thick line) and without persistent sodium channels (thin line). The intensity of the conditioning current was for both models set to 40% of the threshold of the test stimulus alone. The model without persistent sodium current was obtained by leaving out persistent sodium channels in the new model of paper IV. The figure is taken from paper IV.

The model in paper IV with persistent sodium current reproduced threshold electrotonus and a close resemblance between the underlying electrotonic changes in membrane potential and threshold electrotonus was found (see Figure 17). However, when the persistent sodium current was removed the electronic changes still resembled the electrotonic changes with persistent sodium current, but threshold electrotonus did not parallel the underlying electrotonic changes in membrane potential (see Figure 17). This behavior of the model is the same as what was observed in the study of Baker and Bostock (1989) (2). Consequently, the model predicts a relation between persistent sodium channels and both threshold electrotonus and breakdown of accommodation. A second prediction of the model is that the threshold only parallels the electrotonic changes in membrane potential when the nerve fiber exhibit breakdown of accommodation.

5.5   Implications for sub-threshold prepulses

Hill's theory of accommodation predicts that the intensity of a ramp prepulse can be set to any value if its slope is below the critical slope of the nerve (48). Thus, in theory, ramp prepulses should be more efficient than rectangular prepulses for selective electrical stimulation. However, in practice the difference between ramp and rectangular prepulses may be minor, as breakdown of accommodation implies that there is no critical slope for ramp prepulses (11;62). Breakdown of accommodation, will imposes a constraint on the effectiveness of prepulses, as it will set a limit to how much the threshold of the undesired fiber groups can be increased. Based on this limit it is likely that prepulses only will be effective for selective activation of nerve fibers within relatively homogeneous fiber groups (such as α-motor neurons) or nerve fibers confined in small regions.

6 Possible applications

The results of paper I, suggests that the concept of deactivating functions can be used to design electrodes for selective stimulation methods that relies on accommodation (today, exponentially rising waveforms and sub-threshold prepulses). The electrodes should be designed so there is the maximum difference between the deactivating function of the nerve fibers to be blocked and the nerve fibers to be selectively stimulated. This approach has the advantage that linear models can be used for design of electrodes, which considerably reduces the complexity of the analysis.

In paper I, II, and III, exponentially rising waveforms and sub-threshold prepulses were found capable of changing the recruitment order of electrical stimulation. This may facilitate stimulation protocols in functional electrical stimulation that minimize fatigue, either trough alternating between subsets of motor nerves or by preferentially activating slow fatigue resistant motor units. Small motor neurons may be selectively activated with rectangular prepulses, which innervates slow fatigue resistant muscle fibers (24;110). To obtain smooth muscle contractions it is necessary to use stimulation frequencies of 30Hz to 50Hz, but at these frequencies, there is rapid fatigue of the activated motor units (92). By switching between stimuli with and without rectangular prepulses or between rectangular and exponentially rising stimuli, it may be possible to stimulate with the high frequencies needed for smooth muscle contractions while only stimulating each individual motor unit with half of that frequency. Consequently, the fatigue of the activated muscles units may be reduced. To reach that end, more research in intelligent stimulators are needed, to develop stimulators that can monitor the electrical evoked responses to the stimuli so the stimulation parameters can be adjusted in order to obtain the desired effect.

Threshold electrotonus and other threshold tracking methods represent a major intellectual achievement, as it can be applied in clinical studies on humans and it gives information that can be directly related to membrane properties (19). However, it relies on the assumption of a close correspondence between threshold and membrane potential. This assumption is warranted in normal physiological conditions (3;23), but it is not warranted in ischaemic conditions (2). Unfortunately, for obvious reasons it is not possible to assess the validity of this assumption in human studies using measurements of thresholds and membrane potentials. This would require intra-cellular recordings, which involves extensive surgery and is likely to be a destructive process. The results of paper IV suggest that measurement of breakdown of accommodation may be used to assess the validity of the assumption of threshold to be an index of membrane potential.

7 Conclusions

A) A theoretical explanation has been obtained for the selective activation of small nerve fibers with slowly rising and exponentially rising waveforms. Hence, propagation of action potentials evoked by exponentially rising waveforms fail for lower stimulus intensities in large nerve fibers than in small nerve fibers. This was explained by a larger second order difference quotient of the membrane potential (which was termed deactivating function) for large nerve fibers than for small nerve fibers. This allowed selective activation of small nerve fibers in a model of a nerve enclosed by a cuff electrode (Paper I).

B) Rectangular prepulses of short and long duration were compared in an animal model. It was concluded that there was no effect of increasing the duration of rectangular prepulses from 1ms to 10ms or 100ms (Paper II).

C) Ramp prepulses were observed to be effective for selective activation of both small and distant nerve fibers in human experiments. The results of paper I, III, and IV, suggested that the effect of prepulses cannot be described solely by sodium inactivation. Instead, it was suggested that their effect is dependent on a number of both linear and non-linear mechanisms that either decrease or increase the excitation threshold, and that breakdown of accommodation impose a limit to the effectiveness of prepulses, which may restrict their use to relatively homogeneous fiber groups (Paper I, III, IV).

D) Breakdown of accommodation can be explained by persistent sodium current, that has been found theoretically to create a "threshold region" of membrane depolarization, which cannot be exceeded without the generation of action potentials (Paper IV).

References

1. Accornero N, Bini G, Lenzi GL, Manfredi M. Selective Activation of peripheral nerve fibre groups of different diameter by triangular shaped stimulus pulses. J.Physiol 1977;273(3):539-60.

2. Baker M, Bostock H. Depolarization changes the mechanism of accommodation in rat and human motor axons. J.Physiol 1989;411:545-61.

3. Baker M, Bostock H, Grafe P, Martius P. Function and distribution of three types of rectifying channel in rat spinal root myelinated axons. J.Physiol 1987;383:45-67.

4. Baker MD. Selective block of late Na(+) current by local anaesthetics in rat large sensory neurones. Br.J.Pharmacol. 2000;129(8):1617-26.

5. Baker MD, Bostock H. Low-threshold, persistent sodium current in rat large dorsal root ganglion neurons in culture. J.Neurophysiol. 1997;77(3):1503-13.

6. Baker MD, Bostock H. Inactivation of macroscopic late Na+ current and characteristics of unitary late Na+ currents in sensory neurons. J.Neurophysiol. 1998;80(5):2538-49.

7. Baker MD, Bostock H. The pH dependence of late sodium current in large sensory neurons. Neuroscience 1999;92(3):1119-30.

8. Baratta R, Ichie M, Hwang SK, Solomonow M. Orderly stimulation of skeletal muscle motor units with tripolar nerve cuff electrode. IEEE Trans.Biomed.Eng 1989;36(8):836-43.

9. Barrett EF, Barrett JN. Intracellular recording from vertebrate myelinated axons: mechanism of the depolarizing afterpotential. J.Physiol 1982;323:117-44.

10. Behse F. Morphometric studies on the human sural nerve. Acta Neurol.Scand.Suppl 1990;132:1-38.

11. Bernhard CG, Granit R, Skoglund CR. The breakdown of accommodation - nerve as a model sense-organ. J.Neurophysiol. 1942;5:55-68.

12. Berthold CH, Nilsson I, Rydmark M. Axon diameter and myelin sheath thickness in nerve fibres of the ventral spinal root of the seventh lumbar nerve of the adult and developing cat. J.Anat. 1983;136 (Pt 3):483-508.

13. Berthold CH, Rydmark M. Morphology of normal peripheral axons. In: Waxman SG, Kocsis JD, Stys PK, editors. The Axon. Oxford University Press, Inc.; 1995. p. 49-67.

14. Blair E, Erlanger J. A comparison of the charactheristics of axons through their individual electrical responces. Am.J.Physiol. 1933;106:524-64.

15. Blumenthal TD, Burnett TT, Swerdlow CD. Prepulses reduce the pain of cutaneous electrical shocks. Psychosom.Med. 2001;63(2):275-81.

16. Bostock H. The strength-duration relationship for excitation of myelinated nerve: computed dependence on membrane parameters. J.Physiol 1983;341:59-74.

17. Bostock H, Baker M, Reid G. Changes in excitability of human motor axons underlying post-ischaemic fasciculations: evidence for two stable states. J.Physiol 1991;441:537-57.

18. Bostock H, Burke D, Hales J. Differences in behaviour of sensory and motor axons following release of ischaemia. Brain 1994;117:225-34.

19. Bostock H, Cikurel K, Burke D. Threshold tracking techniques in the study of human peripheral nerve. Muscle Nerve 1998;21(2):137-58.

20. Bostock H, Rothwell JC. Latent addition in motor and sensory fibres of human peripheral nerve. J.Physiol 1997;498 (Pt 1):277-94.

21. Bostock H, Sears TA. The internodal axon membrane: electrical excitability and continuous conduction in seqmental demyelination. J.Physiol.(Lond.) 1978;280:273-301.

22. Bowman BR, McNeal DR. Response of Single Alpha Motorneurons to High-Frequency Pulse Trains, Firing Behavior and Conduction Block Phenomenon. Appl.Neurophysiol. 1986;49:121-38.

23. Burke D, Kiernan MC, Bostock H. Excitability of human axons. Clin.Neurophysiol. 2001;112(9):1575-85.

24. Burke RE, Levine DN, Tsairis P, Zajac FE, III. Physiological types and histochemical profiles in motor units of the cat gastrocnemius. J.Physiol 1973;234(3):723-48.

25. Caldwell JH, Schaller KL, Lasher RS, Peles E, Levinson SR. Sodium channel Na(v)1.6 is localized at nodes of ranvier, dendrites, and synapses. Proc.Natl.Acad.Sci.U.S.A 2000;97(10):5616-20.

26. Chiu SY, Ritchie JM, Rogart RB, Stagg D. A quantitative description of membrane currents in rabbit myelinated nerve. J.Physiol 1979;292:149-66.

27. Dengler R, Stein RB, Thomas CK. Axonal conduction velocity and force of single human motor units. Muscle Nerve 1988;11:136-45.

28. Deurloo KE, Holsheimer J, Bergveld P. The effect of subthreshold prepulses on the recruitment order in a nerve trunk analyzed in a simple and a realistic volume conductor model. Biol.Cybern. 2001;85(4):281-91.

29. Deurloo KEI, Boere CJP, Jong EJ, Holsheimer J. Optimization of Inactivation Current Waveform for Selective Peripheral Nerve Stimulation. Proceedings of the Second Annual IFESS Conference (IFESS'97) and Neural Prothesis: Motor Systems 5 (NP'97) 1997:237-8.

30. Dreyer SJ, Dumitru D, King JC. Anodal block V anodal stimulation. Fact or fiction. Am.J.Phys.Med.Rehabil. 1993;72(1):10-8.

31. Dumitru D. Electrodiagnostic Medicine. Yeong Mun Publishing Company; 1994.

32. Eng DL, Gordon TR, Kocsis JD, Waxman SG. Development of 4-AP and TEA sensitivities in mammalian myelinated nerve fibers. J.Neurophysiol. 1988;60:2168-79.

33. Fang ZP, Mortimer JT. A method to effect physiological recruitment order in electrically activated muscle. IEEE Trans.Biomed.Eng 1991;38(2):175-9.

34. Fang ZP, Mortimer JT. Selective activation of small motor axons by quasi-trapezoidal current pulses. IEEE Trans.Biomed.Eng 1991;38(2):168-74.

35. Feiereisen P, Duchateau J, Hainaut K. Motor unit recruitment order during voluntary and electrically induced contractions in the tibialis anterior. Exp Brain Res 2004;114:117-23.

36. Foster RE, Conners BW, Waxman SG. Rat optic nerve: Electrophysiological, pharmacological, and anatomical studies during development. Dev.Brain Res. 1982;3:361-76.

37. Frankenhauser B, Huxley AF. The Action Potential In The Myelinated Nerve Fibre of Xenopus Laevis As Computed On The Basis Of Voltage Clamp Data. J.Physiol 1964;171:302-15.

38. Fukushima K, Yahara O, Kato M. Differential blocking of motor fibers by direct current. Pflugers Arch. 1975;358(3):235-42.

39. Godfrey S, Butler JE, Griffin L, Thomas CK. Differential Fatigue of Paralyzed Thenar Muscles by Stimuli of Different Intensities. Muscle Nerve 2002;26:122-31.

40. Grill WM, Mortimer JT. Stimulus Waveforms for Selective Neural Stimulation. IEEE Engineering in Medicine and Biology 1995:375-85.

41. Grill WM, Mortimer JT. Inversion of the current-distance relationship by transient depolarization. IEEE Trans.Biomed.Eng 1997;44(1):1-9.

42. Grill WM, Jr., Mortimer JT. The effect of stimulus pulse duration on selectivity of neural stimulation. IEEE Trans.Biomed.Eng 1996;43(2):161-6.

43. Halter J, Clark J. A distributed-parameter model of the myelinated nerve fiber. J.Theor.Biol. 1991;148:345-82.

44. Helliwell TR, Coakley J, Smith PE, Edwards RH. The morphology and morpometry of the normal human tibialis anterior muscle. Neuropathol.Appl.Neurobiol. 1987;13:297-307.

45. Henneman E. Recruitment of motorneurons: the size principle. Prog.Clin.Neurophysiol. 1981;9:26-60.

46. Hennings K, Andersen OK, Struijk JJ, Arendt-Nielsen L. Modeling Selective Activation of Thin Nerve Fibers using Exponentially Rising Waveforms. 7th Annual Conference of the International Functional Electrical Stimulation Society: 2002.

47. Henriksson-Larsen KJ, Whetling M. Distribution of fiber sizes in human skeletal muscle. An enzyme histochemical study in muscle tibialis anterior. Acta Physiol Scand. 1985;123:171-7.

48. Hill AV. Excitation and accommodation in nerve. Proc.R.Soc. 1936;119:305-55.

49. Hodgkin AL, Huxley AF. A quantitative description of membrane current and its application to conduction and excitation in nerve. Bull.Math.Biol. 1952;52(1-2):25-71.

50. Ingram DA, Davis GR, Swash M. Motor nerve conduction velocity distribution in man: results of a new computer-based collision technique. Electroencephalogr.Clin.Neurophysiol. 1987;66:235-43.

51. Ingram DA, Davis GR, Swash M. The double collision technique: a new method for measurement of the motor nerve refractory period distribution in man. Electroencephalogr.Clin.Neurophysiol. 1987;66:225-34.

52. Jakobsson E, Guttman R. The standard Hodgkin-Huxley model and squid axons in reduced external Ca++ fail to accommodate to slowly rising currents. Biophys.J. 1980;31(2):293-7.

53. Kandel ER, Schwarts JH, Jessell TM. Principles of neural science. 4ed. McGraw-Hill; 2000.

54. Kiernan MC, Burke D, Andersen KV, Bostock H. Multiple measures of axonal excitability: a new approach in clinical testing. Muscle Nerve 2000;23(3):399-409.

55. Kiernan MC, Lin CS, Andersen KV, Murray NM, Bostock H. Clinical evaluation of excitability measures in sensory nerve. Muscle Nerve 2001;24(7):883-92.

56. Kilgore KL, Bhadra N. Nerve conduction block utilising high-frequency alternating current. Med.Biol.Eng Comput. 2004;42:394-406.

57. Knaflitz M, Merletti R, De Luca CJ. Inference of motor unit recruitment order in voluntary and electrically elicited contractions. J.Appl.Physiol. 1990;68(4):1657-67.

58. Kocsis JD, Eng DL, Gordon TR, Waxman SG. Functional differences between 4-AP and TEA-sensitive potassium channels in mammalian axons. Neurosci.Lett. 1987;75:193-8.

59. Kocsis JD, Waxman SG. Intra-axonal recordings in rat dorsal column axons: membrane hyperpolarization and decreased excitability precede the primary afferent depolarization. Brain Res. 1982;238(1):222-7.

60. Kocsis JD, Waxman SG, Hildebrand C, Ruiz JA. Regenerating mammalian nerve fibers: Changes in action potential waveform and firing characteristics following blockage of potassium conductance. Proc.R.Soc.Lond.B 1982;217:277-87.

61. Kuffler SW, Vaughan-Villiams EM. Small nerve junctional potentials. The distribution of small motor nerves to frog skeletal muscle, and the membrane characteristics of the fibres they innervate. J.Physiol 1953;121:289-317.

62. Kugelberg E. Accommodation in human nerves. Acta Physiol.Scand. 1944;8 (suppl. 24):1-115.

63. Kugelberg E, Skoglund CR. Natural and artificial activation of motor units - A comparison. J.Neurophysiol. 1946;9:399-412.

64. Lucas K. On the rate of variation of the exciting current as a factor in electrical excitation. J.Physiol.(Lond.) 1907;36:253-74.

65. Manfredi M. Differential block of conduction of larger fibers in peripheral nerve by direct current. Arch.Ital.Biol. 1970;108(1):52-71.

66. McIntyre CC, Richardson AG, Grill WM. Modeling the excitability of mammalian nerve fibers: influence of afterpotentials on the recovery cycle. J.Neurophysiol. 2002;87(2):995-1006.

67. McNeal DR. Analysis of a model for excitation of myelinated nerve. IEEE Trans.Biomed.Eng 1976;23(4):329-37.

68. MCPHEDRAN AM, WUERKER RB, Henneman E. PROPERTIES OF MOTOR UNITS IN A HETEROGENEOUS PALE MUSCLE (M. GASTROCNEMIUS) OF THE CAT. J.Neurophysiol. 1965;28:85-99.

69. Merletti R, Knaflitz M, De Luca CJ. Myoelectric manifestations of fatigue in voluntary and electrically elicited contractions. J.Appl.Physiol 1990;69(5):1810-20.

70. Nilsson HJ, Levinsson A, Schouenborg J. Cutaneous field stimulation (CFS): a new powerful method to combat itch. Pain 1997;71(1):49-55.

71. Nilsson I, Berthold CH. Axon classes and internodal growth in the ventral spinal root L7 of adult and developing cats. J.Anat. 1988;156:71-96.

72. Panizza M, Nilsson J, Bradley JR, Rothwell JC, Hallett M. The time constants of motor and sensory peripheral nerve fibers measured with the method of latent addition. Electroencephalogr.Clin.Neurophysiol. 1994;93:147-54.

73. Panizza M, Nilsson J, Roth BJ, Grill SE, Demirci M, Hallett M. Differences between the time constant of sensory and motor peripheral nerve fibers: further studies and considerations. Muscle Nerve 1998;21(1):48-54.

74. Patlak J. Molecular kinetics of voltage-dependent Na+ channels. Physiol Rev. 1991;71(4):1047-80.

75. Poletto CJ, Van Doren CL. Elevating pain thresholds in humans using depolarizing prepulses. IEEE Trans.Biomed.Eng 2002;49(10):1221-4.

76. Rattay F. Analysis of models for external stimulation of axons. IEEE Trans.Biomed.Eng 1986;33(10):974-7.

77. Rattay F. Analysis of models for extracellular fiber stimulation. IEEE Trans.Biomed.Eng 1989;36(7):676-82.

78. Rattay F. Electrical Nerve Stimulation: Theory, Experiments and Applications. Springer-Verlag; 1990.

79. Rattay F, Aberham M. Modeling axon membranes for functional electrical stimulation. IEEE Trans.Biomed.Eng 1993;40(12):1201-9.

80. Reid G, Scholz A, Bostock H, Vogel W. Human axons contain at least five types of voltage-dependent potassium channel. J.Physiol 1999;518 (Pt 3):681-96.

81. Rijkhoff NJ, Holsheimer J, Debruyne FM, Wijkstra H. Modelling selective activation of small myelinated nerve fibres using a monopolar point electrode. Med.Biol.Eng Comput. 1995;33(6):762-8.

82. Rijkhoff NJ, Holsheimer J, Koldewijn EL, Struijk JJ, van Kerrebroeck PE, Debruyne FM et al. Selective stimulation of sacral nerve roots for bladder control: a study by computer modeling. IEEE Trans.Biomed.Eng 1994;41(5):413-24.

83. Ruijten MWMM, Sallé HJA, Kingma R. Comparison of two techniques to measure the motor nerve conduction velocity distribution. Electroencephalogr.Clin.Neurophysiol. 1993;89:375-81.

84. Rydmark M. Nodal axon diameter correlates linearly with internodal axon diameter in spinal roots of the cat. Neurosci.Lett. 1981;24(3):247-50.

85. Rydmark M, Berthold CH. Electron microscopic serial section analysis of nodes of Ranvier in lumbar spinal roots of the cat: a morphometric study of nodal compartments in fibres of different sizes. J.Neurocytol. 1983;12(4):537-65.

86. Röper J, Schwarz JR. Heterogeneous distribution of fast and slow potassium channels in myelinated rat nerve fibers. J.Physiol.(Lond.) 1989;416:93-110.

87. Safronov BV, Kampe K, Vogel W. Single voltage-dependent potassium channels in rat peripheral nerve membrane. J.Physiol.(Lond.) 1993;460:675-91.

88. Sassen M, Zimmermann M. Differential blocking of myelinated nerve fibres by transient depolarization. Pflugers Arch. 1973;341(3):179-95.

89. Scholz A, Reid G, Vogel W, Bostock H. Ion channels in human axons. J.Neurophysiol. 1993;70(3):1274-9.

90. Schwarz JR, Eikhof G. Na currents and action potentials in rat myelinated nerve fibres at 20 and 37 degrees C. Pflugers Arch. 1987;409(6):569-77.

91. Schwarz JR, Reid G, Bostock H. Action potentials and membrane currents in the human node of Ranvier. Pflugers Arch. 1995;430(2):283-92.

92. Solomonow M. External Control of the Neuromuscular System. IEEE Trans.Biomed.Eng 1984;31(12):752-63.

93. Stephanova DI. Myelin as longitudinal conductor: a multi-layered model of the myelinated human motor nerve fibre. Biol.Cybern. 2001;84(4):301-8.

94. Sunderland S. Nerves and nerve injuries. Churchill Livingstone; 1978.

95. Sweeney JD, Mortimer JT, Durand D. Modeling of mammalian myelinated nerve for functional neuromuscular stimulation. Boston: 1987.

96. Tai C, Jiang D. Selective stimulation of smaller fibers in a compound nerve trunk with single cathode by rectangular current pulses. IEEE Trans.Biomed.Eng 1994;41(3):286-91.

97. Tanner JA. Reversible Blocking of Nerve Conduction by Alternating-Current Excitation. Nature 1962;195:712-3.

98. Tasaki I. New measurements of the capacity and the resistance of the myelin sheath and the nodal membrane of the isolated frog nerve fiber. Am.J.Physiol. 1955;181:639-50.

99. Thomas CK, Broton JG, Calancie B. Motor Unit Forces and Recruitment Patterns after Cervical Spinal Cord Injury. Muscle Nerve 1997;20:212-20.

100. Thomas CK, Johansson RS, Westling G, Bigland-Ritchie B. Twitch Properties of Human Thenar Motor Units Measured in Response to Intraneural Motor-Axon Stimulation. J.Neurophysiol. 1990;64(4):1339-46.

101. Thomas CK, Nelson G, Than L, Zijdewind I. Motor Unit Activation Order During Electrically Evoked Contractions of Paralyzed or Partially Paralyzed Muscles. Muscle Nerve 2002;25:797-804.

102. Trenchard D, Widdicombe JG. Assessment of differential block of conduction by direct current applied to the cervical vagus nerve. Acta Neurobiol.Exp.(Warsz.) 1973;33(1):89-96.

103. Trimble MH, Enoka RM. Mechanisms Underlying the Training Effects Associated with Neuromuscular Electrical Stimulation. Physical Therapy 1991;71(4):273-82.

104. Vabnick I, Trimmer JS, Schwarz TL, Levinson SR, Risal D, Shrager P. Dynamic potassium channel distributions during axonal development prevent aberrant firing patterns. J.Neurosci. 1999;19:747-58.

105. van Bolhuis AI, Holsheimer J, Savelberg HH. A nerve stimulation method to selectively recruit smaller motor-units in rat skeletal muscle. J.Neurosci.Methods 2001;107(1-2):87-92.

106. Veraart C, Grill WM, Mortimer JT. Selective control of muscle activation with a multipolar nerve cuff electrode. IEEE Trans.Biomed.Eng 1993;40(7):640-53.

107. Vuckovic A, Rijkhoff NJ, Struijk JJ. Different Pulse Shapes to Obtain Small Fiber Selective Activation by Anodal Blocking - A Simulation Study. IEEE Trans.Biomed.Eng 2004;51(5):698-706.

108. Wesselink WA, Holsheimer J, Boom HB. A model of the electrical behaviour of myelinated sensory nerve fibres based on human data. Med.Biol.Eng Comput. 1999;37(2):228-35.

109. Yang Q, Kaji R, Hirota N, Kojima Y, Takagi T, Kohara N et al. Effect of maturation on nerve excitability in an experimental model of threshold electrotonus. Muscle Nerve 2000;23(4):498-506.

110. Zajac FE, Faden JS. Relationship Among Recruitment Order, Axonal Conduction Velocity, and Muscle-Unit Properties of Type-Identified Motor Units in Cat Plantaris Muscle. J.Neurophysiol. 1985;53(5):1303-22.

111. Zengel JE, Reid SA, Sypert GW, Munson JB. Membrane Electrical Properties and Prediction of Motor-Unit Type of Medial Gastronemius Motorneurons in the Cat. J.Neurophysiol. 1985;53(5):1323-44.

112. Zimmermann M. Selective activation of C-fibers. Pflugers Arch.Gesamte Physiol Menschen.Tiere. 1968;301(4):329-33.